# GENERAL GEOLOGY AND THE PREDICTION OF LIMESTONE GEOHAZARD USING ELECTRICAL RESISTIVITY IMAGING (ERI) AT GUA MADU, GUA MUSANG, KELANTAN

by

**Abdul Hakim Bin Yahaya**
**E13A002**

A report submitted in fulfillment of the requirements for the degree of Bachelor of Applied Science (Geoscience) with Honours

**FACULTY OF EARTH SCIENCE**
**UNIVERSITI MALAYSIA KELANTAN**

2017

FYP FSB
UNIVERSITI MALAYSIA KELANTAN

## DECLARATION

I hereby declare that the work embodied in this report is the result of the original research and has not been submitted for a higher degree to any universities of institutions.

…….

Student

Name: Abdul Hakim b Yahaya

Date: 4th December 2016

FYP FSB
UNIVERSITI MALAYSIA KELANTAN

FYP FSB

## ACKNOWLEDGEMENT

In the name of Allah, the Most Gracious and the Most Merciful

Alhamdulillah, all praise to Allah for strengths and His blessing in completing this proposal. Special appreciation goes to my supervisor, Miss Zakiyah bt Ainul Kamal, for her supervision and constant support. Her invaluable help of constructive comments and suggestions throughout the thesis works have contributed to the success of this research.

I would like to express my appreciation to all lab assistant and office staff of University Malaysia Kelantan for their co-operation, support and help towards my research.

Sincere thanks to all my friends for their kindness and moral support during my study. Thanks for the friendship and memories.

Last but not least, my deepest gratitude goes to my beloved parents; Yahaya b Md Sah and Siti Salmah bt Osman for their endless love, prayers and encouragement. To those who indirectly contributed in this research, your kindness means a lot to me.

UNIVERSITI MALAYSIA KELANTAN

## TABLE OF CONTENTS


| | | PAGE |
|---|---|---|
| **DECLARATION** | | **ii** |
| **ACKNOWLEDGEMENT** | | **iii** |
| **ABSTRACT** | | **vii** |
| **ABSTRAK** | | **viii** |
| **LIST OF TABLES** | | **ix** |
| **LIST OF FIGURES** | | **x** |
| **LIST OF ABBREVIATIONS** | | **xiii** |
| **LIST OF SYMBOLS** | | **xiv** |
| **CHAPTER 1** | **INTRODUCTION** | |
| 1.1 | General Background | 1 |
| 1.2 | Problem Statements | 4 |
| 1.3 | Research Objectives | 5 |
| 1.4 | Study Area | 5 |
| 1.4.1 | Location | 5 |
| 1.4.2 | Rainfall distribution | 7 |
| 1.4.3 | Social economic | 7 |
| 1.4.4 | Accessibility | 8 |
| 1.5 | Scope of Study | 10 |
| 1.6 | Research Importances | 10 |
| **CHAPTER 2** | **LITERATURE REVIEW** | |
| 2.1 | Introduction | 11 |
| 2.2 | Regional Geology and Tectonic Setting | 11 |
| 2.2.1 | Stratigraphy | 12 |
| 2.2.2 | Structural Geology | 12 |
| 2.2.3 | Historical Geology | 13 |




FYP FSB
UNIVERSITI MALAYSIA KELANTAN

2.3 Electrical Resistivity Imaging (ERI) 14
2.3.1 Resistivity Array 19
2.4 Limestone 21
2.5 Limestone Geohazard 22

**CHAPTER 3 MATERIALS AND METHODS**

3.1 Introduction 24
3.2 Materials 26
3.3 Methodology 27
3.3.2 Field studies 28
3.3.3 Laboratory investigations 28
3.3.3 Data processing 29
3.3.4 Data analysis and interpretation 29

**CHAPTER 4 GENERAL GEOLOGY**

4.1 Introduction 30
4.2 Geomorphology 30
4.2.1 Traverse map 32
4.2.2 Drainage pattern map 32
4.2.3 Drainage catchment area 34
4.2.4 Topographic map 39
4.2.5 Weathering process 42
4.2.6 Landslide 45
4.3 Petrography
4.3.1 Study Area 52
4.4 Stratigraphy 72
4.5 Structural Geology 74
4.5.1 Linearment analysis 74
4.5.2 Joint analysis 77
4.6 Historical Geology 84

**CHAPTER 5 ELECTRICAL RESISTIVITY IMAGING ANALYSIS**



FYP FSB
UNIVERSITI MALAYSIA KELANTAN

5.1 Introduction 85
5.2 Electrical Resistivity Profile 87
5.3 Analysis 89
5.4 Result 92
5.4.1 P1 93
5.4.2 P2 95
5.4.3 P3 97

**CHAPTER 6 CONCLUSION AND RECOMMENDATION**

6.1 Conclusion 99
6.2 Recommendation 100

References 101
Appendices 104

FYP FSB
UNIVERSITI MALAYSIA KELANTAN

**General Geology and Prediction of Limestone Geohazard using Electrical Resisticity Imaging (ERI) at Gua Madu, Gua Musang, Kelantan**

## ABSTRACT

This study is about the general geology and prediction of limestone geohazard by using electrical resistivity imaging at Gua Madu, Gua Musang, Kelantan. The purpose of this study is to enhance the geological map of study area to scale 1:25000 and to assess limestone geohazard of the study area. The geological map is enhanced by geological mapping , field observation and sampling of rocks. The rocks sample is cut into thin section for petrography analysis. Reading of joints in strike and dip is taken for structural analysis. To assess the limestone geohazard of the study area, electrical resistivity imaging (ERI) method is selected. By using the ERI method, subsurface voids are found at the target area. There are three electrical resistivity profiles labelled P1, P2 and P3. P1 and P2 shows that these area is very stable due to the presence of massive limestone underground and high resistivity value detected. P3 shows that the risk of potential limestone geohazard to occur is high based on the undergroundwater found and low resistivity value in the area. The overall results from this study indicate that the study area is stable and the risk of potential limestone geohazard to occur is low.

FYP FSB
UNIVERSITI MALAYSIA KELANTAN

**Geologi Am dan Ramalan Geobencana Batu Kapur Menggunakan Pengimejan Rintangan Elektrik di Gua Madu, Gua Musang, Kelantan**


## ABSTRAK

Kajian ini adalah mengenai geologi am dan ramalan geobencana batu kapur menggunakan pengimejan rintangan elektrik di Gua Panjang, Gua Musang, Kelantan. Tujuan kajian ini dilakukan adalah untuk menambah baik peta geologi dalam skala 1:25000 dan untuk menilai kemungkinan geobencana batu kapur di kawasan kajian. Peta geologi dihasilkan dengan pemetaan geologi, pemerhatian di lapangan dan mengambil sampel batuan. Sampel batuan yang diambil dipotong dan digunakan untuk menghasilkan slaid keratan nipis yang digunakan untuk tujuan analisis petrografi. Bacaan strike dan dip struktur batuan diambil untuk kajian struktural. Untuk menilai geobencana batu kapur, kaedah pengimejan rintangan elektrik telah dipilih. Dengan pengimejan rintangan elektrik, ruang kosong di bawah permukaan kajian dapat ditemui. Terdapat tiga profil rintangan elektrik dilabel sebagai P1, P2 and P3. P1 dan P2 menunjukkan bahawa kawasan sekitar adalah stabil dengan bukti saiz batu kapur yang besar bawah tanah beserta dengan nila rintangan yang tinggi. P3 menunjukkan bahawa kemungkinan geobencana batu kapur untuk berlaku adalah tinggi kerana terdapat bukti air bawah tanah dan nilai rintangan yang rendah di kawasan sekitar. Hasil daripada kajian ini menunjukkan bahawa kawasan kajian adalah stabil dan potensi geobencana batu kapur untuk berlaku adalah rendah.



FYP FSB

UNIVERSITI MALAYSIA KELANTAN

## LIST OF TABLES


| NO | TITLE | PAGE |
|---|---|---|
| 4.1 | Dunham's classification | 51 |
| 4.2 | Stratigraphic column of study area | 73 |
| 4.3 | Joint sampling reading (location 1) | 80 |
| 4.4 | Joint sampling reading (location 2) | 81 |
| 4.5 | Joint sampling reading (location 3) | 82 |
| 4.6 | Joint sampling reading (location 4) | 83 |


FYP FSB

UNIVERSITI MALAYSIA KELANTAN

## LIST OF FIGURES


| NO | TITLE | PAGE |
|---|---|---|
| 1.1 | A huge sinkhole caused by a burst water pipe is seen at Jalan Imbi in Kuala Lumpur, July 2, 2014. | 4 |
| 1.2 | Base map of the study area | 7 |
| 1.3 | Graph illustrating trend of rainfall in Gua Musang | 8 |
| 1.4 | Gate near Forest Department | 9 |
| 2.1 | Flow of current from a point current source and the resulting potential distribution | 17 |
| 2.2 | Schematic diagram of a multielectrode system used for a 2 – D electrical survey and an example sequence of measurements used to build up a pseudo section | 18 |
| 2.3 | Common arrays used in the resistivity surveys | 19 |
| 2.4 | The resistivity of rocks, soils and minerals | 20 |
| 2.5 | Formation of different types of sinkholes | 24 |
| 2.6 | Karst formation | 24 |
| 3.1 | Equipment used for electrical imaging resistivity (ERI) | 27 |
| 4.1 | Drainage network patterns | 34 |
| 4.2 | Traverse map | 37 |
| 4.3 | Drainage pattern of study area | 38 |
| 4.4 | Drainage catchment area | 39 |
| 4.5 | 2D Topographic Map | 41 |
| 4.6 | 3D topographic map | 42 |
| 4.7 | Effect of biological weathering that occurs at Gua Madu | 45 |
| 4.8 | Effect of physical weathering that can be seen near Gua Madu | 45 |
| 4.9 | Types of landslide | 47 |




FYP FSB
UNIVERSITI MALAYSIA KELANTAN

| | | |
|---|---|---|
| 4.10 | Slump at Kampung Batu Papan | 48 |
| 4.11 | Earthflow near Perhentian Gua Musang | 48 |
| 4.12 | Earthflow at Taman Wangi | 49 |
| 4.13 | Rock fall near the main road to Kampung Batu Papan | 49 |
| 4.14 | Folk's classification | 51 |
| 4.15 | QAPF diagram for classification and nomenclature of plutonic igneous rocks | 52 |
| 4.16 | Outcrop Station for each sample | 54 |
| 4.17 | Location of outcrop at station 1 | 56 |
| 4.18 | Hand specimen of outcrop at station 1 | 56 |
| 4.19 | Location of outcrop at station 2 | 60 |
| 4.20 | Hand specimen of outcrop at station 2 | 60 |
| 4.21 | Location of outcrop at station 3 | 63 |
| 4.22 | Hand specimen of outcrop at station 3 | 63 |
| 4.23 | Location of outcrop at station 4 | 67 |
| 4.24 | Hand specimen of outcrop at station 4 | 67 |
| 4.25 | Location of outcrop at station 5 | 70 |
| 4.26 | Hand specimen of outcrop at station 5 | 70 |
| 4.27 | Geological map of study area | 74 |
| 4.28 | Lineament of study area | 76 |
| 4.29 | Rose diagram of lineament reading | 77 |
| 4.30 | Joint sampling map | 79 |
| 4.31 | Rose diagram of location 1 | 80 |
| 4.32 | Rose diagram of location 2 | 81 |
| 4.33 | Rose diagram of location 3 | 82 |




FYP FSB
UNIVERSITI MALAYSIA KELANTAN

| | | |
|---|---|---|
| 4.34 | Rose diagram of location 4 | 83 |
| 4.35 | Rose diagram of all joint sampling data combined | 84 |
| 5.1 | The resistivity of rocks, soils and minerals | 87 |
| 5.2 | ERI Profile location of study area | 89 |
| 5.3 | Example of a data set with a few bad data points | 91 |
| 5.4 | Product of inversion using least square inversion method | 92 |
| 5.5 | Trimming with cut-off error selected at 15% | 93 |
| 5.6 | Resistivity profile P1 | 94 |
| 5.7 | Resistivity profile P2 | 96 |
| 5.8 | Resistivity profile P3 | 98 |


FYP FSB

UNIVERSITI
MALAYSIA
KELANTAN

## LIST OF ABBREVIATION

| | |
|---|---|
| JUPEM | Jabatan Ukur dan Pemetaan Malaysia |
| JKR | Jabatan Kerja Raya |
| JMG | Jabatan Mineral dan Geologi |
| ERI | Electrical Resistivity Imaging |

FYP FSB
UNIVERSITI MALAYSIA KELANTAN

## LIST OF SYMBOLS

| | |
|---|---|
| J | Current Density |
| $\sigma$ | Conductivity of the medium |
| E | Electric field intensity |
| $\rho$ | Resistivity |

.

FYP FSB

UNIVERSITI
MALAYSIA
KELANTAN

# CHAPTER 1

# INTRODUCTION

## 1.1 General Background

The study area is located at the Gua Madu, where many limestone hills are present. It is located at the east coast of Kelantan. It is surrounded mainly by forest reserved, river and hills. The average elevation of Gua Madu area is 200 metres. It is located 3 km to the south from the Gua Musang town. Gua Madu is one of the limestone caves that are present in this area.

At Gua Madu, massive limestone hills are present in the midst of a lowly urbanised area. The Gua Madu is embellished by majestic high relief limestone hills and decorated with many limestone morphological features such as caves and dolines. However, most of the limestone hills are mainly characterized by adverse structural conditions such as joints and fractures.

Geologic hazards include such things as existing landslides or areas prone to landslides, the presence of acid producing rock, soft or weak soil, old abandoned mine sites, contaminated ground, caves and sinkhole areas. Caves and sinkholes which form from the karst formation, can give challenges relative to both the physical and environmental issues of highway development.



FYP FSB
UNIVERSITI MALAYSIA KELANTAN

There are many limestone formations in Malaysia. In Peninsular Malaysia, the major occurrences are in Klang Valley, Kinta Valley, Kedah-Perlis (including the Langkawi Islands), Kelantan (Gua Musang area), and Pahang. In these areas, limestone occurs as a majestic, precipitous cliffs as well as extensive bedrock formations. No limestone hills occur in the southern regions of Peninsular Malaysia (Johor, Melaka)

A recent high-rise project in the K.L. area witnessed the tremendous efforts put in to detect the cavities in the limestone bedrock by employing 100 boreholes on a close-grid pattern. Numerous cavities, some at multi-levels, were detected through those efforts. Much of KL is built along limestone areas and there are many cavities underground. It is estimated that a third of Kuala Lumpur is built on limestone bedrock. Sinkholes tend to occur with such a geological formation.

One sinkhole happened the morning of 2 July 2014, at the junction of Jalan Pudu - Jalan Imbi - Jalan Hang Tuah ( Figure 1.2 ). This is the junction of the old Pudu prison, Police headquarters and Times Square. The sinkhole was said to be 20 m deep. The cause was said to be a burst water pipe. The collapse covers a 19 m stretch and is just 20 m from the elevated monorail. The study area consists of limestone area and very similar to this area.

FYP FSB
UNIVERSITI MALAYSIA KELANTAN

**Figure 1.1** : A huge sinkhole caused by a burst water pipe is seen at Jalan Imbi in Kuala Lumpur, July 2, 2014. ( Source : The Malay Online )

## 1.2 Problem Statements

This research is made in order to collect the data from Gua Madu area. Rapid developments of the area render the available geological map absolute. The latest geological map of Gua Madu was published in sheet by Jabatan Ukur Dan Pemetaan Malaysia (JUPEM) on 1993 with revision done on 1995 and 2004. Since then, the geological map has not been update for about 12 years.

The limestone is a sedimentary rock composed of calcium carbonate ($CaCO_3$) minerals that when exposed to acidic water, will dissolved and leach way. The acidic water can be from acid rain and carbonic acid. This can cause development of subsurface cavities that in time can collapse and cause subsidence and sinkholes.

The potential limestone geohazard can cause destruction if it is not taking care of by the authorities and people living in that area. Furthermore, the map of the area is outdated. It must be up to date with the latest features. To do that, a geological mapping must be done in that area to identify the new features to update the map.

No details research has been done in the study area. Electrical Resistivity Imaging (ERI) is one of the methods to identify the subsurface condition at Gua Madu. This is important as the occurrence of limestone in this area can potentially turn into limestone geohazards.

## 1.3 Research Objectives

The main objective for the research proposal:

i. To enhance the geological map of the study area in the scale of 1:25000
ii. To identify subsurface condition by using electrical resistivity imaging (ERI)
iii. To predict limestone geohazard potential in the study area

## 1.4 Study Area

### 1.4.1 Location

The study area covers 25 $km^2$ (5 km x 5 km) surrounding Gua Madu within the location ( 4° 49.2' - 4°52.0' ) N and ( 101° 55.15 - 101° 58.3') E. As shown in Figure 1.3. Within the study area, there is part of Gua Madu cave limestone karst at the southeast of the map. Electrical Resistivity Imaging (ERI) will be conduct surrounding of the limestone. Figure 1.1 shows the base map of the study area.



FYP FSB
UNIVERSITI MALAYSIA KELANTAN

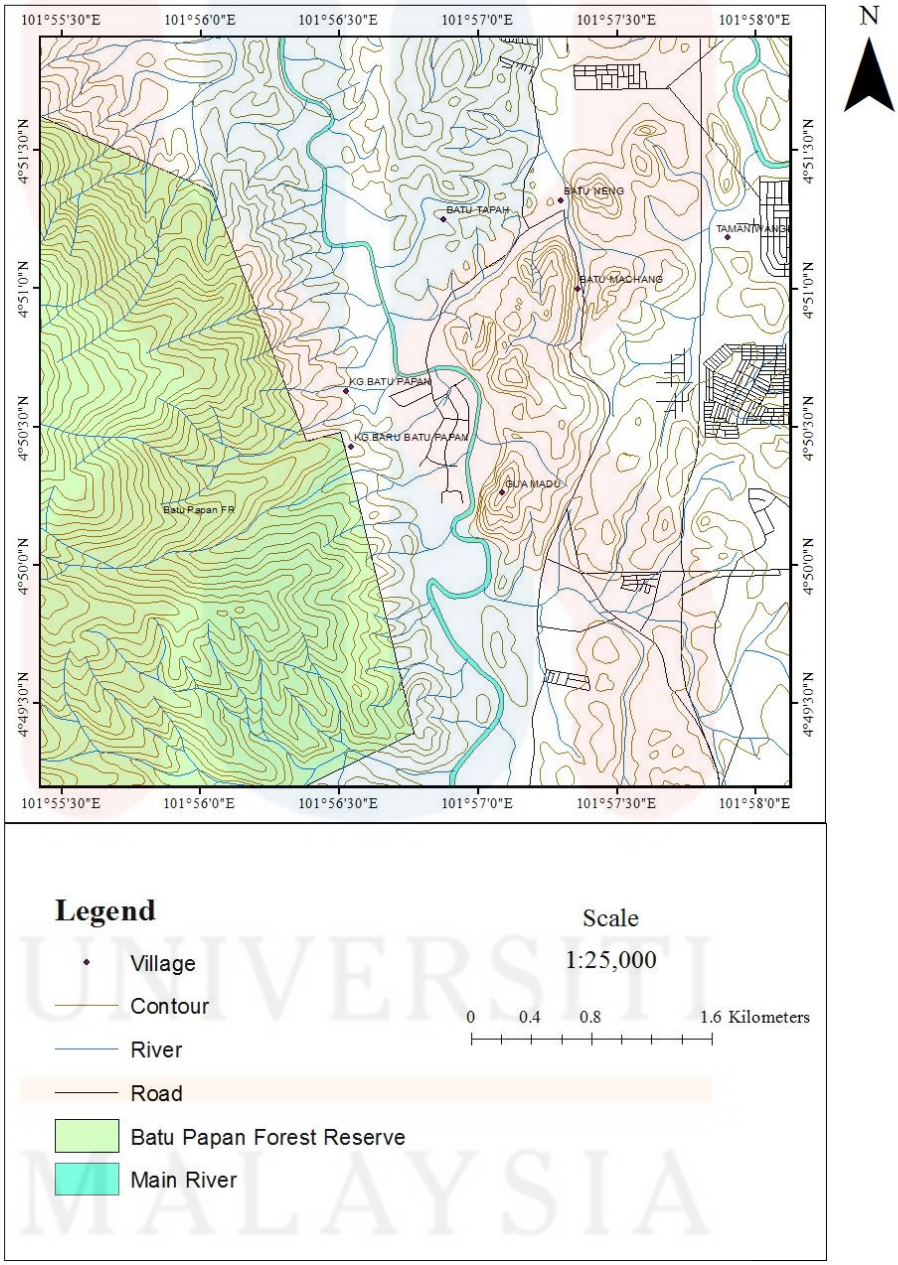


**Figure 1.3** : Base map of the study area

### 1.4.2 Rainfall distribution

In Figure 1.4, the graph shows rainfall data in selected range. The data is from the year 2005 to 2014. In the year 2014, the rainfall rate reaches all-time high, causes the worst flood in the history of Kelantan.

**Figure 1.3** : Graph illustrating trend of rainfall in Gua Musang

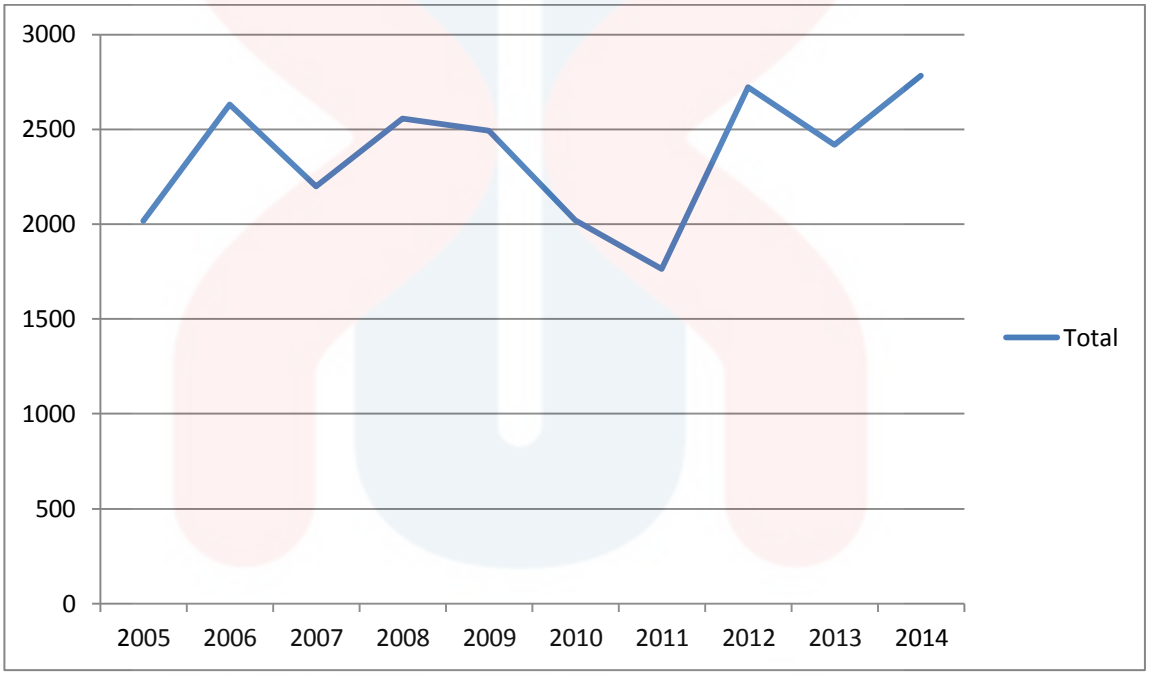


### 1.4.3 Social economic

In the study area, the social economic income mainly come from plantation. This is due to the higher number of plantation area that present in the area, such as rubber and palm oil plantation. Some of the people doing animal husbandry like breeding cows, goats and chicken.

### 1.4.4 Accessibility

There are two ways to access the study area by vehicle. First is near the Forest Department Gate ( N 4° 50’ 01.34” E 101° 57’ 11.3”) in Figure 1.4. At the crossroads, take exit to the right. Another way is through Kampung Batu Papan. At the end of Kg Batu Papan road, there is a small hanging bridge that can only be access by motorcycle ( N 4°50'13.0" E 101°56'55.1") in Figure 1.5.

**Figure 1.4**: Gate near Forest Department ( Source : Google Earth )

FYP FSB
UNIVERSITI MALAYSIA KELANTAN

**Figure 1.5** : Small hanging bridge as an entrance to the study area

## 1.5 Scope of Study

The scope of the study is to investigate the potential of limestone geohazard using electrical resistivity imaging (ERI). Electrical resistivity imaging (ERI) will shows resistivity data of the study area by measuring the subsurface condition using ABEM Terameter SAS 4000. Electrical resistivity imaging starts with the collection of data by using series of electrodes placed on the surface. The size and resolution of an image is defined by the distance between electrodes and their location in space. The data gathered can used to create three subsurface profiles for the limestone area.

FYP FSB
UNIVERSITI MALAYSIA KELANTAN

## 1.6 Research Importance

First is updating the map. A new, updated and latest map was produced at the end of the resarch. This map can be used as a future reference by other researcher who wants to know more about the area. Other institutions such as Jabatan Kerja Raya (JKR) can refer to the map when they want to build new roads. Jabatan Mineral & Geologi (JMG) can use the map to possibly conserve the geological features in the area.

The new, updated geological map contains more information about the Gua Madu area. The descriptions of those units or materials can be transferred into useful geohazards mapping. For example, maps that show the limestone formation exposed at the surface also represent areas subject to karst development. With this information, person such as an engineer can estimate the safest place he or she wanted to construct buildings or infrastructure. Furthermore, a preliminary data can be produced as a guide for future references.

FYP FSB
UNIVERSITI
MALAYSIA
KELANTAN

# CHAPTER 2

# LITERATURE REVIEW

## 2.1 Introduction

This chapter discussed in detail the geology of the region which is Peninsular Malaysia, its tectonic setting, and its history. The electrical resistivity also is studied based on its past usage in similar field of study, its advantages and disadvantages compare to other geophysical method, its operation method and data processing method.

## 2.2 Regional Geology and Tectonic Setting

Peninsular Malaysia is a part of 'Sundaland', which is a part of the Eurasian Plate. The Sunda Shelf is the extension of the peninsula eastwards and southwards. Sumatra, Natuna, and western Borneo, that belong on the same plate ( Hutcinson, 1973 )

Due to convergence at Sunda Trench, the Sumatra Island is dominated by dextral wrench faults. Also, a dextral wrench fault occurred at Andaman sea marginal basin resulting in southward movement called as Sumatran Fault System, and northward movement called Sagaing Fault.



FYP FSB
UNIVERSITI MALAYSIA KELANTAN

The Malaysian peninsular is different to Sarawak tectonically and stratigraphically, but is similar to Indonesian Island of Bangka. Hutchinson proposed that Sarawak geology should be similar to the Vietnam.

### 2.2.1 Stratigraphy

Gua Musang is a town and territory in Kelantan, Malaysia. It is the largest district in Kelantan. Gua Musang is administered by the Gua Musang District Council. Gua Musang district is bordered by the state of Pahang to the south, Terengganu to the east, Perak to the west and the Kelantanese districts of Kuala Krai and Jeli to the north. It is a small railway town about 160 kilometres south of Kuala Krai.

On the eastern side of this town stands Bukit Gua Musang, a barren hill of rocks and deceptive stone-steps running 105 meters high. It stands in a commanding position, with a huge cave running into its interior and is about meters away from the other green tree-covered hills. From a distance, this hill looks like a stone pillar with a big crack which nearly splits it vertically into two equal halves.

### 2.2.2 Structural Geology

Structural geology is the study of structure of rocks at all scales and the process involved in producing those structures. Tectonic setting is the one of the main process that can cause structural geology to perform. Peninsular Malaysia was formed by the collision between Sinoburmalaya to the west and Eastmal-Indonesia blocks to the east forming Peninsular Malaysia. Bentong Raub structure represents the collision zone



FYP FSB
UNIVERSITI MALAYSIA KELANTAN

which it can be traced northwest into Thailand and southeast into the Banka and Biliton Islands.

The major tectonic event during late Triassic which has resulted in rock deformation in the Malay-Thai Peninsula has been associated in these collisions. Series of synclines and anticlines has been observed in the transect area of pre-orogeny sedimentary successions. The character folding is tight, asymmetric and open folds, resulting in the repeated and overturned sequence in the older sedimentary rock.

The trending fold axes of northwest-southwest and north-south are sub parallel to the long axis of the Malay Peninsula and most of the bedding planes show dipping towards the east with various dip angles. Fault zones are exposed at more than a few places along the trace. It varies with their width characterized by the fractured, sheared or mylonitised rocks ( The Malaysia and Thai Working Groups, 2006 ).

### 2.2.3 Historical Geology

The formation at the study area is Gua Musang Formation. The formation age ranges from the Middle Permian to Upper Triassic, covering parts of Paleozoic era and Mesozoic era (Mohd Shafeea Leman, 2007). The limestone occurs as lenses and forms isolated towers of limestone, and 650 meters thick.

The Paleozoic stratigraphy of the Gua Musang Formation comprises of crystalline limestone interbedded with thin shale, tuff, chert nodules, and sandstone. The limestone at the formation has black and grey variety. This comes from the impurities of carbonaceous, argillaceous and pyroclastic origin.



FYP FSB
UNIVERSITI MALAYSIA KELANTAN

## 2.3 Electrical Resistivity Imaging (ERI)

A course in geophysics should appeal to geology majors as well as physics majors. Geology majors will have expectations of such a course that are different from the expectations of physics students (Parker and Whittles, 1970). A section of a geophysics course studying electrical resistivity has recently been described in this journal (Avants, Soodak, and Ruppeiner,1999).

Electrical resistivity studies in geophysics may be understood in the context of current flow through a subsurface medium consisting of layers of materials with different individual resistivity (Reynolds,1997). Some of the examples that are using this technique are bedrock fracture zones, fault zones, delineating tunnels and cavernous zones, contamination plumes, characterizing landfills, water table determination and archeological investigations.

Electrical resistivity techniques were used in cave detection (Cook and Nostrand, 1954; Vincenz, 1968; Dutta et al., 1970; Greenfield, 1979; Militzer et al., 1979; Smith, 1986 ). Thomas and Roth (1999) presented a comparison study between 12 methods (including four geophysical techniques) for sinkhole and void detection. Hutchinson et al. (2002) provided a useful comparison of various geophysical approaches for void detection. Contribution of geophysical methods to karst-system exploration was completed by Chalikakis et al. (2011). Cardarelli et al. (2006a) use electrical resistivity tomography to detect buried cavities in Rome.

2D resistivity imaging requires data to be recorded with many different electrode separations along a line. It is important to have a dense enough data cover laterally and



FYP FSB
UNIVERSITI MALAYSIA KELANTAN

in terms of electrode separations to recover complex structures in the ground (e.g. Griffiths and Barker, 1993; Dahlin and Loke, 1998), which demands the use of automated multi-electrode data acquisition systems to be practical. The direct current resistivity method uses a man-made apparatus source of electrical current that is injected into the earth through grounded electrodes. The resulting potential field is measured along the ground using a second pair of electrodes. The transmitting and receiving electrode pairs are referred to as dipoles.

By varied the unit length of the dipoles as well as the distance between them, the horizontal and vertical distribution of electrical properties can be recorded. Determination of the effective depth of the boundary between the two layers may be performed using the so-called ‘‘cumulative resistivity’’ method. This method employs a plot of the sum of the apparent resistivity versus the effective depth (E. S. Robinson and C. Coruh, 1988).

The fundamental physical law used in resistivity surveys is Ohm’s Law that governs the flow of current in the ground. The equation for Ohm’s Law in vector form for current flow in a continuous medium is given by:

$$\boldsymbol{J = \sigma E}$$

where $\sigma$ is the conductivity of the medium, J is the current density and E is the electric field intensity. In practice, the electric field potential is measured. In geophysical surveys the medium’s resistivity, $\rho$ which is equals to the reciprocal of the conductivity is used.



FYP FSB
UNIVERSITI MALAYSIA KELANTAN

There are two electrical based methods that are closely related to the resistivity method. They are the Induced Polarization (IP) method, and the Spectral Induced Polarization (SIP) method. Both methods require measuring instruments that are more sensitive than the normal resistivity method, as well has significantly higher currents. Both IP and SIP surveys use alternating currents of much higher frequencies than standard resistivity surveys. Electromagnetic coupling is a serious problem in both methods. To minimize the electromagnetic coupling, the dipole-dipole (or pole-dipole) array is commonly used.

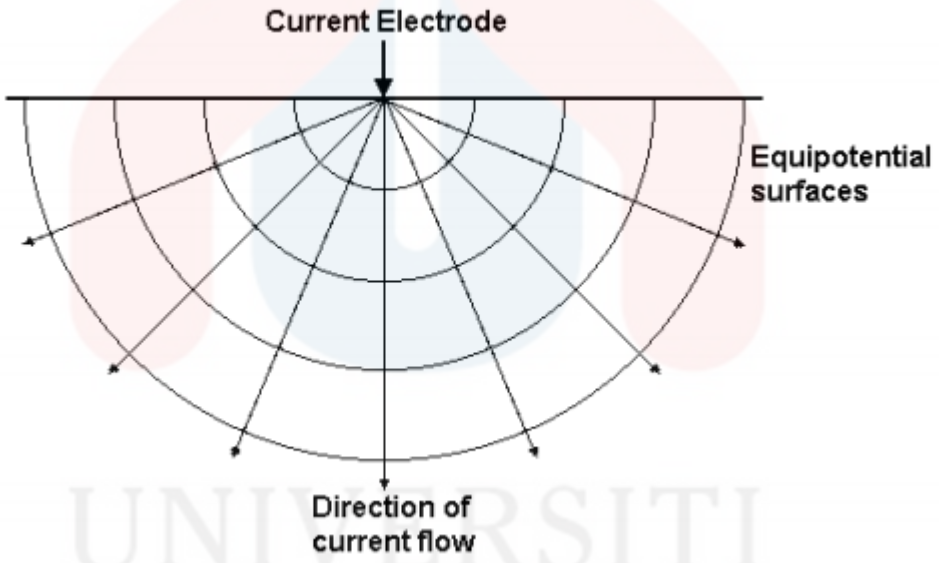


**Figure 2.1** : Flow of current from a point current source and the resulting potential distribution ( from Loke 2014 )

The instrument type can be divided into two broad categories, static and dynamic systems. Most instruments are of the static type where many electrodes are connected to a multi-electrode cable and planted into the ground during the. One common configuration is a split spread type of cable connection to the switching unit at the centre

to reduce the individual cable length and weight. A common spacing used for most engineering and environmental surveys is 5 meters.

Most systems come with a minimum of 28 nodes, with some system having up to 128 nodes or more. To obtain a good 2-D picture of the subsurface, the coverage of the measurements must be 2-D as well. As an example, Figure 2.1 shows a possible sequence of measurements for the Wenner electrode array for a system with 20 electrodes.

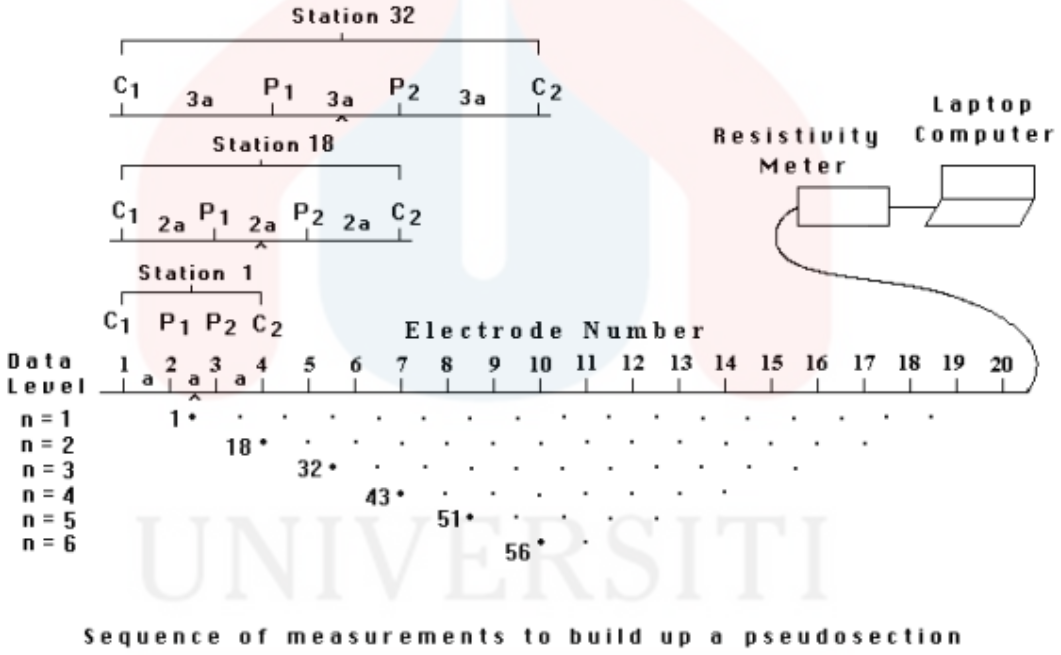


**Figure 2.2**: Schematic diagram of a multielectrode system used for a 2 – D electrical survey and an example sequence of measurements used to build up a pseudo section ( Source : http://www.landviser.net )

There are several ways in which the electrodes in Figure 2.2 may be arranged, with the spacing chosen to match the needs of a particular survey site. Some of these arrangements are pictured in Fig. 2.3. Each of these electrode configurations has its own

advantages and disadvantages, depending on the type of survey to be performed. There are 4 main types of array : Wenner array, Schlumberger array, pole – pole array, dipole – dipole array.

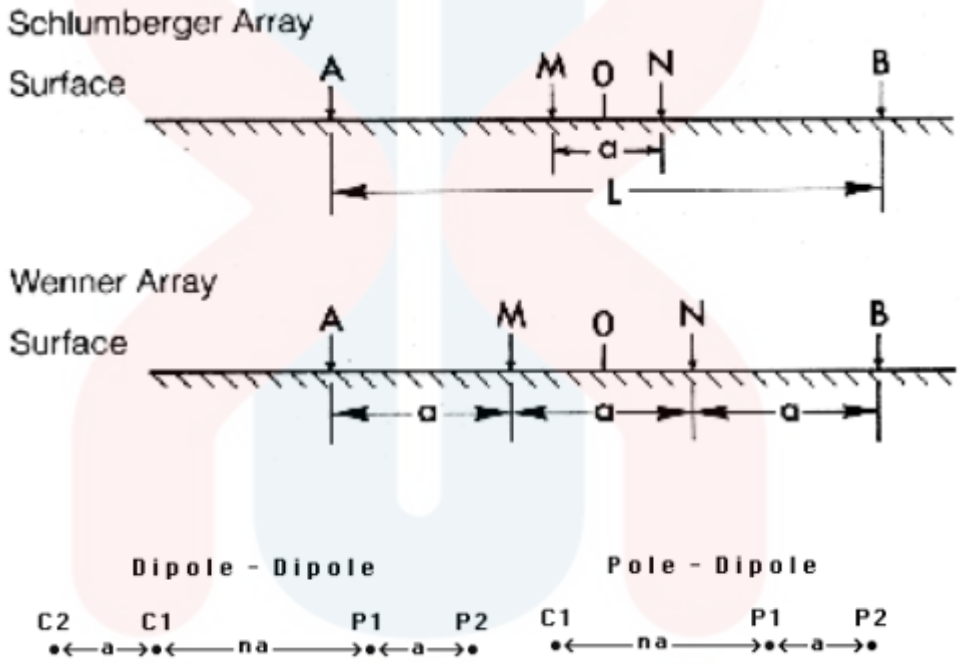


**Figure 2.3** : Common arrays used in the resistivity surveys

( Source : http://www.landviser.net )

Electric current flows in earth materials at shallow depths through two main methods. They are electronic conduction and electrolytic conduction. In electronic conduction, the current flow is via free electrons, such as in metals. In electrolytic conduction, the current flow is via the movement of ions in groundwater. The resistivity of common rocks, soil materials and chemicals (Keller and Frischknecht 1966, Daniels

and Alberty 1966, Telford et al. 1990) is shown in Figure 2.4. Igneous and metamorphic rocks typically have high resistivity values.

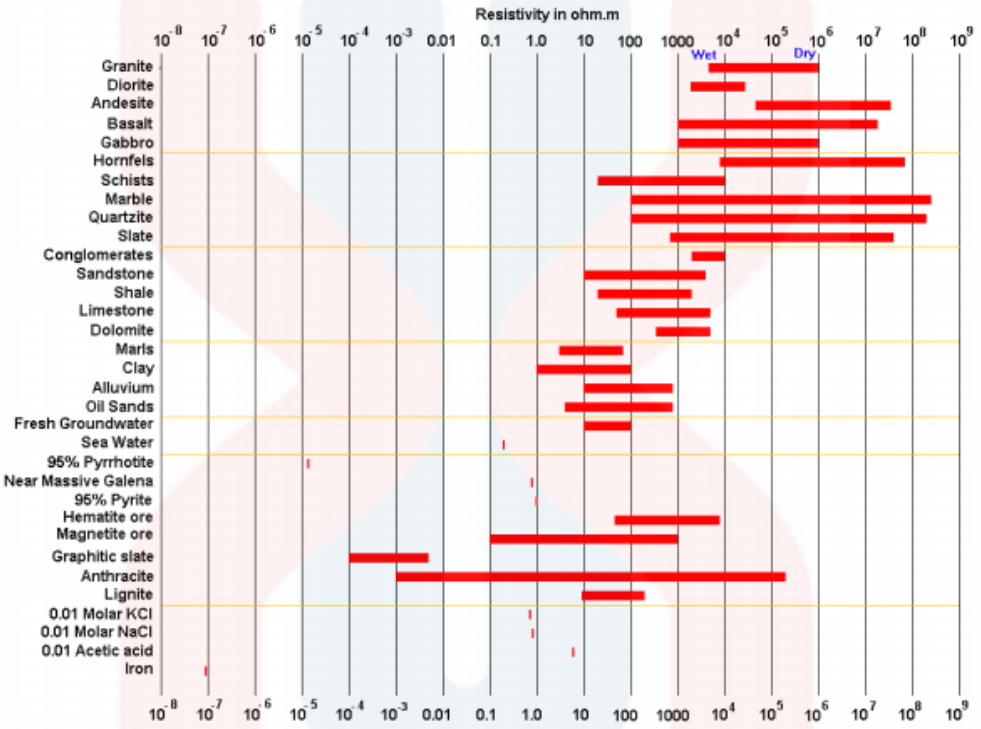


**Figure 2.4**: The resistivity of rocks, soils and minerals ( from Loke 2014 )

### 2.3.1 Resistivity Array

The arrays most commonly used for resistivity surveys were shown in Figure 2.3. The choice of the "best" array for a field survey depends on the type of structure to be mapped, the sensitivity of the resistivity meter and the background noise level. In practice, the arrays that are most commonly used for 2-D imaging surveys are the (a) Wenner, (b) dipole-dipole (c) Wenner-Schlumberger (d) pole-pole and (d) pole-dipole. Among the characteristics of an array that should be considered are (i) the sensitivity of

the array to vertical and horizontal changes in the subsurface resistivity, (ii) the depth of investigation, (iii) the horizontal data coverage and (iv) the signal strength.

a) Wenner array

This is a robust array that was popularized by the pioneering work carried by The University of Birmingham research group (Griffiths and Turnbull 1985; Griffiths, Turnbull and Olayinka 1990). Many of the early 2-D surveys were carried out with this array. The sensitivity plot for the Wenner array has almost horizontal contours beneath the centre of the array. Because of this property, the Wenner array is relatively sensitive to vertical changes in the subsurface resistivity below the centre of the array.

b) Dipole-dipole array

This array has still widely used in resistivity surveys because of the low E.M. coupling between the current and potential circuits. The arrangement of the electrodes is shown in Figure 2.3. This array is most sensitive to resistivity changes between the electrodes in each dipole pair.

c) Wenner – Sclumberger array

This is a new hybrid between the Wenner and Schlumberger arrays (Pazdirek and Blaha 1996) arising out of relatively recent work with electrical imaging surveys. The classical Schlumberger array is one of the most commonly used array for resistivity sounding surveys.



FYP FSB
UNIVERSITI MALAYSIA KELANTAN

The sensitivity pattern for the Schlumberger array is slightly different from the Wenner array with a slight vertical curvature below the centre of the array. This means that this array is moderately sensitive to both horizontal and vertical structures. In areas where both types of geological structures are expected, this array might be a good compromise between the Wenner and the dipole-dipole array.

d) Pole-pole array

This array is not as commonly used as the Wenner, dipole-dipole and Schlumberger arrays. In practice the ideal pole-pole array, with only one current and one potential electrode in Figure 2.3, does not exist. this array is mainly used in surveys where relatively small electrode spacings less than 10 metres are used. It is popular in some applications such as archaeological surveys where small electrode spacings are used. It has also been used for 3-D surveys (Li and Oldenburg 1992).

e) Pole-dipole array

The pole-dipole array also has relatively good horizontal coverage, but it has a significantly higher signal strength compared with the dipole-dipole array and it is not as sensitive to telluric noise as the pole-pole array. Due to its good horizontal coverage, this is an attractive array for multi-electrode resistivity meter systems with a relatively small number of nodes. The signal strength is lower compared with the Wenner and Wenner-Schlumberger arrays but higher than the dipole-dipole array.

FYP FSB
UNIVERSITI MALAYSIA KELANTAN

## 2.4 Limestone

Limestone means any rock formed mostly of calcium carbonate (CaCO3), but to geologists, limestone is only one of several types of carbonate rocks. These rocks are composed of more than 50% carbonate minerals, generally the minerals calcite (pure CaCO3) or dolomite (calcium-magnesium carbonate) or both. Most carbonate rocks were deposited from seawater. These sedimentary carbonate rocks are common on every continent and have formed through most of geologic history and they are still forming today in the tropics as coral reefs and at the bottoms of shallow seas. (Figure 2.5)

Marine limestone forms because seawater has high concentrations of two key dissolved chemicals-calcium and bicarbonate ions. In the near-surface layer of most oceans, corals, clams, and other sea-dwelling creatures use these two chemicals to make protective shells by combining them to form calcite or aragonite, which is the same chemical composition as calcite but has a different crystal form.

## 2.5 Limestone Geohazard

Limestone geohazard usually associated with the karst formation ( Figure 2.6). Karst is a distinctive topography in which the landscape is largely shaped by the dissolving action of water on carbonate bedrock (usually limestone, dolomite, or marble). This geological process, occurring over many thousands of years, results in unusual surface and subsurface features ranging from sinkholes, vertical shafts, disappearing streams, and springs, to complex underground drainage systems and caves.



FYP FSB
UNIVERSITI MALAYSIA KELANTAN

The process of karst formation ( Figure 2.7 ) involves what is referred to as "the carbon dioxide cascade." As rain falls through the atmosphere, it picks up carbon dioxide which dissolves in the droplets. Once the rain hits the ground, it percolates through the soil and picks up more carbon dioxide to form a weak solution of carbonic acid. The infiltrating water naturally exploits any cracks or crevices in the rock.

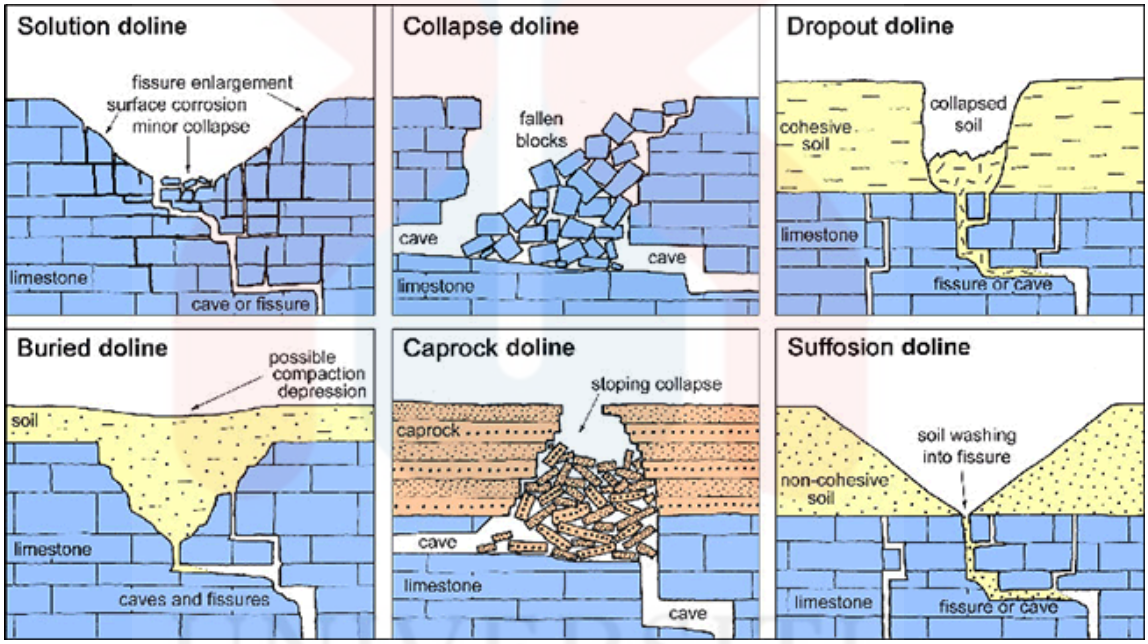


**Figure 2.5** : Formation of different types of sinkholes ( Source : http://www.bgs.ac.uk )

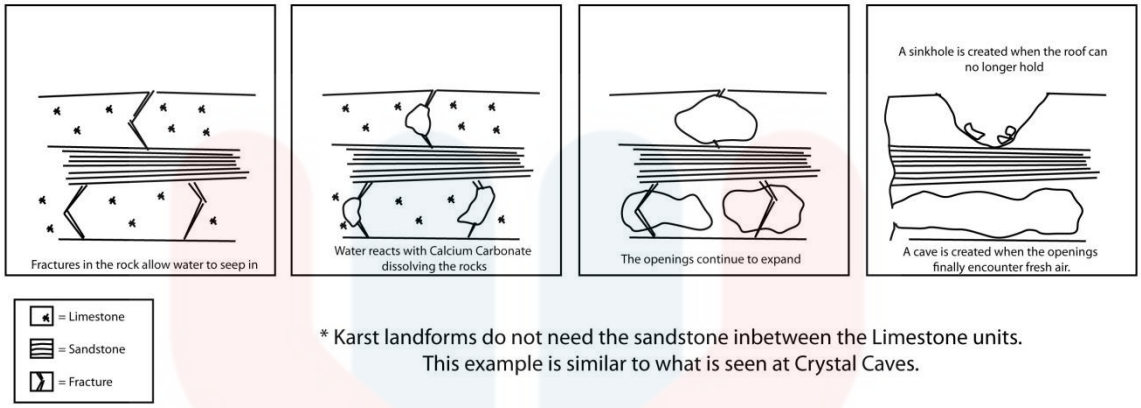


**Figure 2.6** : Karst formation ( Source : http://people.uwec.edu)

FYP FSB
UNIVERSITI MALAYSIA KELANTAN

# CHAPTER 3

# MATERIALS AND METHODOLOGY

## 3.1 Introduction

The electrical resistivity imaging (ERI) technology employed in this research was developed as a response to the standard techniques used for characterizing and monitoring environmental sites. The second strategy uses indirect measurements through surface or borehole geophysical techniques. The difficulties with point sampling are the cost and time of drilling; and sample collection, analysis, and interpretation time. Further, point sampling methods typically provide low data density and thus miss contaminants transported on flow paths or stored in clay lenses not sampled by wells.

The large amounts of data produced by multielectrode systems require automated data handling and processing. Automatic inverse numerical modelling techniques (inversion) based on the finite difference or finite element methods for the forward calculations have been developed in response to this need (e.g. Oldenburg and Li, 1994; Tsourlos, 1995; Loke and Barker, 1996a).

FYP FSB
UNIVERSITI MALAYSIA KELANTAN

This is especially problematic if the contaminants are moving non-uniformly, such as density-driven fingering or in isolated flow paths in heterogeneous media. Various approximate schemes have been presented to reduce the large computational efforts associated with the sensitivity matrix used in adjusting the model, e.g. the quasi Newton method (Loke and Barker, 1996a), but these are generally most suitable for small resistivity contrasts.

## 3.2 Materials

The equipment needed for the research :

**Figure 3.1** : Equipment used for electrical imaging resistivity (ERI)

1. Global Positioning System (GPS)
2. Electrical survey
3. Electrodes
4. Multi-core cable
5. Resistivity meter

## 3.3 Methodology

Method of Electrical Resistivity Imaging (ERI)

Electrical resistivity imaging begins with data acquisition using a series of electrodes placed either on the surface or in boreholes. Two-dimensional data is collected using a linear array of electrodes while three-dimensional data can be collected using electrodes placed as a two-dimensional array or as a three-dimensional electrode grid. The size and resolution of an image is defined by the distance between electrodes and their location in space. A rough estimate for a two dimensional image is that the resolution is half of the electrode spacing and the image depth is one fifth of the total surface line length.

FYP FSB
UNIVERSITI MALAYSIA KELANTAN

Method to Produce Geological Map

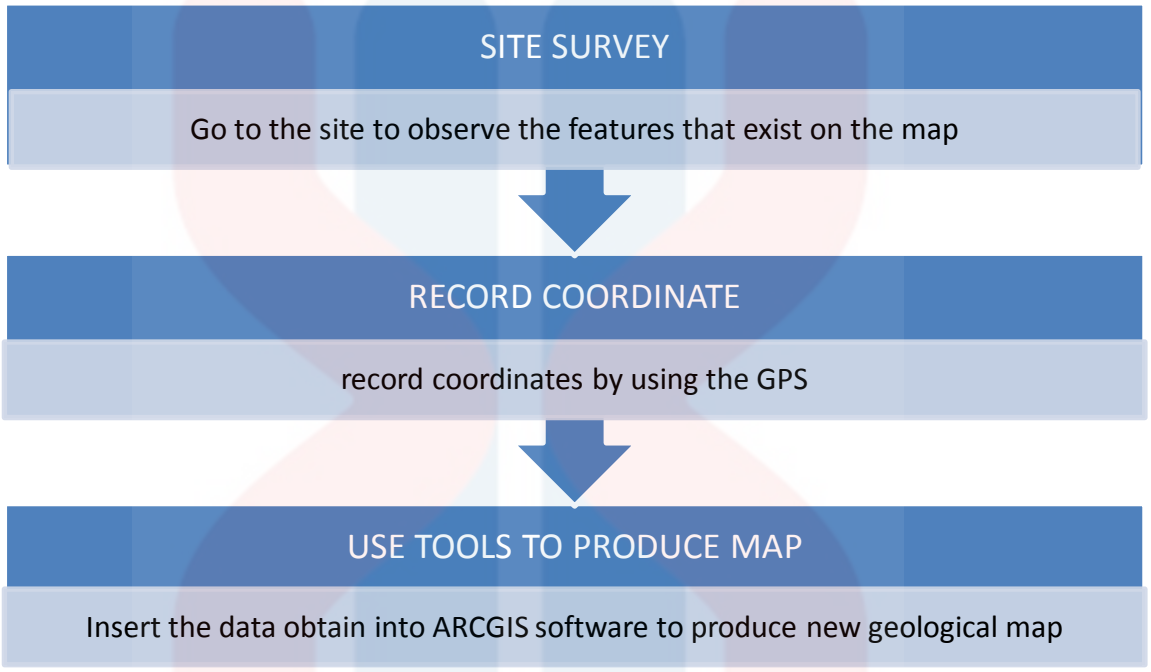


### 3.3.1 Field Studies

The field study is dividing into two parts, one is the geological aspect of the area by geological mapping and the other one is about the specification of the study, which is electrical resistivity imaging (ERI).

The geological mapping is done to review the maps of the study area, to confirm the lithology type and to check the drainage pattern change. The activity is partially guided by the work done by (Lisle, Brabham & Barnes, 2011) in their book, *Basic Geological Mapping*.

The electrical resistivity method is going to be done at 200 metres using ABEM Terrameter LS. The location of ERI profile is determined by the analysis of satellite imagery, ability to accommodate desired length, and accessibility Array type is considered according to each level pros and cons.

### 3.3.2 Laboratory Investigations

The laboratory investigation is focused on petrology part. The rock samples taken from the study area is analyzed by the means of thin section petrography. This is done to determine the mineral constituent of the rock, its porosity and any other factors that can influence the dissolution rate of the rock.

### 3.3.3 Data processing

After the field survey, the resistance measurements are reduced to apparent resistivity values. Practically all commercial multi-electrode systems come with the computer software to carry out this conversion. ABEM Terrameter LS Toolbox and RES2DINV software is use for processing data.

### 3.3.4 Data Analysis and Interpretation

The raw data acquired from the field must be converted into suitable format, in order to be inverted. Pseudo-section is cross-sectional contour map. Pseudo-section plot



FYP FSB
UNIVERSITI MALAYSIA KELANTAN

is a way of the result of dipole-dipole and pole-dipole is presented, with penetration depth is represented by electrode spacing (n). Inversion is the process of changing data from ‘normal’ pseudo-sections, into ‘inverted’ pseudo-section, which the vertical component of the plot is in scales of depth.

After the inversion process, the data is trimmed to remove errors in the data values. This is needed in order to reduce the percentage of errors in the model. The data is inverted again until it achieves minimum error percentage.

FYP FSB

UNIVERSITI
MALAYSIA
KELANTAN

# CHAPTER 4

# GENERAL GEOLOGY

## 4.1 Introduction

This chapter covers about the general geology of study area. The information in this chapter is obtained by geological mapping and literature review. General geology of the study area is distributed into geomorphology, petrography, stratigraphy, structural geology and historical geology.

## 4.2 Geomorphology

The study of the nature and origin of landform is known as geomorphology. Geomorphologic processes generate that circulate of sediment in the rock cycle and as a result it will shape the Earth surface. This process is influenced by the drainage system, topography, and rate of weathering in that area.

There are two types of geomorphologic process, endogenic and exogenic. The endogenic and exogenic forces causing physical stresses and chemical actions on earth materials and bringing about changes in the configuration of the surface of the earth. Endogenic processes are large-scale landform building and transforming processes . Its

landforms may be tectonic or structural in origin (Twidale 1971, 1). Diastrophism and volcanism are endogenic geomorphic processes.

Exogenic processes include geological phenomena and processes that originate externally to the earth's surfaces. These processes driven by climatic forces (Scheidegger 1979). Weathering, mass wasting, erosion and deposition are exogenic geomorphic processes.

The study area is primarily consisting of limestone, with some area of granite, sandstone and mudstone. Karst features are noticeable in the area, with much evidence of caves and pinnacles.

The term "karst" applies to a distinctive type of landscape that develops from the dissolving action of water on soluble bedrock. Karst landscapes are characterized by fluted and pitted rock surfaces, sinkholes, sinking streams, springs, subsurface drainage systems, and caves.

The formation of karst landscapes in carbonate bedrock involves the "carbon dioxide (CO2) flow". In this process, rain falls through the atmosphere and picks up CO2, which then dissolves into rain droplets. Once the rain hits and infiltrates the ground, it percolates through the soil and picks up more CO 2 and forms a weak solution of carbonic acid.

This slightly acidic water then exploits any existing joints or fractures in the bedrock, gradually dissolving the bedrock and creating larger openings or conduits for the water to flow through. Over many thousands of years, this process eventually creates



FYP FSB
UNIVERSITI MALAYSIA KELANTAN

underground drainage systems and caves. The age of the karst features is around Palaeozoic era, approximately from 252 to 541 million years ago.

### 4.2.1 Traverse Map

Traverse map is basically a base map of study area combine with the data from global positioning system (GPS). Traverse map is use to record the progress of geological mapping of the study area. In Figure 4.2 shows the tracking data had cover most of the study area on the base map.

### 4.2.1 Drainage Pattern

In geomorphology, drainage system is the pattern formed by streams, rivers and lakes in a drainage basin. Inside a network, different patterns can be observed and related to other geographical factors. In a drainage basin, a number of factors such as topography, soil type, bedrock type, climate and vegetation cover influence input, output and transport of sediment and water (Charlton, 2008). These factors also influence the nature of the pattern of water bodies (Twidale, 2004).

There are several types of drainage pattern. At present, much research has been done on the description of drainage patterns in geography and hydrology (Howard, 1967; Lambert, 1998; Twidale, 2004; Pidwirny, 2006). River segments inside a river network can be organised in five types of drainage pattern (Figure 4.1). Dendritic pattern (Figure



FYP FSB
UNIVERSITI MALAYSIA KELANTAN

4.1a) is the most common form of river system. In a dendritic river system, tributaries of a main river join together in a shape analogous to the twigs of a tree (Lambert, 1998).

Parallel patterns (Ritter, 2003) form where there is a pronounced slope to the surface. Tributary streams tend to stretch out in a parallel like fashion following the slope of the surface (Figure 4.1 b). In a trellis pattern (Figure 4.1 c), the main river flows along a strike valley and smaller tributaries feed into it from the steep slopes on the sides of mountains. These tributaries enter the main river at right angles, causing a trellis-like appearance of the river system.

The rectangular pattern (Figure 4.1 d) is found in regions that have undergone faulting. Movements of the surface due to faulting offset the direction of the stream. As a result, the tributary streams make sharp bends and enter the main stream at high angles. Reticulate drainage patterns (Figure 4.1 e) usually occur on floodplains and deltas where rivers often interlace with each other forming a net (Simon and Gerald, 2004).

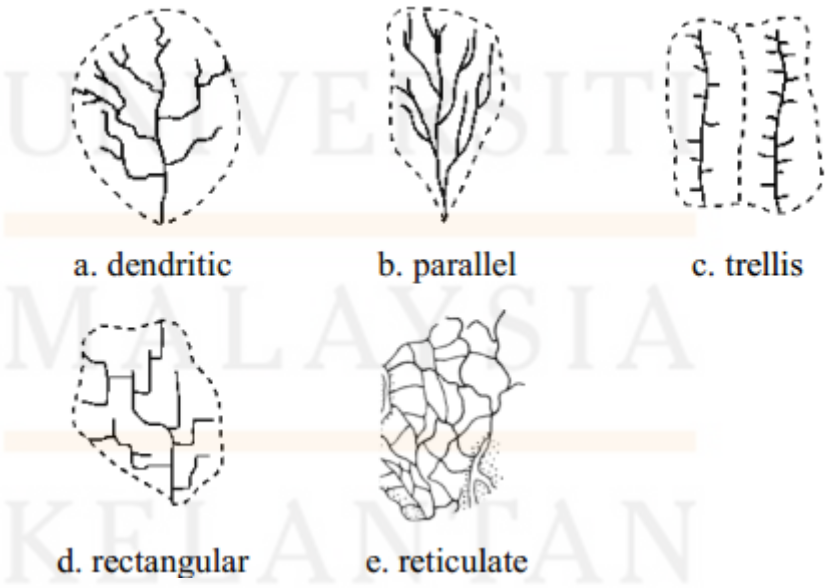


**Figure 4.1** : Drainage network patterns ( diagram modified from Ritter, 2006)

As seen in Figure 4.1, the main river in the study area, Galas River, flows forward Pergau River. The Galas River flow from the N to the S of the map to Kelantan River. There are two drainage patterns that are recognisable in the study area. Label (i) in Figure 4.1 is the parallel drainage pattern and label (ii) in the Figure 4.1 is the dendritic drainage pattern.

### 4.2.2 Drainage Catchment Area

Catchment area is a basin shaped area of land, bounded by natural features such as hills or mountains from which surface and sub-surface water flows into streams, rivers and wetlands. Water flows into, and collects in, the lowest areas in the landscape. The system of streams which transport water, sediment and other material from a catchment is called a drainage network.

A catchment catches water which falls to earth as precipitation (rainfall), and the drainage network channels the water from throughout the catchment to a common outlet. The outlet of a catchment is the mouth of the main stream or river. The mouth may be where it flows into another river or stream, or the place where it empties into a lake or ocean.

Streams begin their journey to the sea in the upper reaches of the catchment. Some may appear briefly, flowing only during periods of intense rainfall. Some are intermittent, flowing during the wet seasons of the year. Others are more permanent, having year-round flow.



FYP FSB
UNIVERSITI MALAYSIA KELANTAN

In the middle reaches of the catchment some tributaries have entered the stream and added to the flow. The land is generally flatter, and the flow of the stream is slower. There are frequent shallow areas of faster moving water called riffles, where rocks break the surface and deeper areas of water called pools. The bottom substrate is composed of mostly gravel and cobble.

Moving downstream towards the streams mouth, more tributaries have entered and added more flow. The wider, deeper channel meanders through a flat flood plain and broad valley. The stream travels very slowly and deposits the large quantities of sediment it has been carrying from further upstream. The catchment area is labelled (i) on the map of study area as seen in Figure 4.3.

FYP FSB
UNIVERSITI
MALAYSIA
KELANTAN

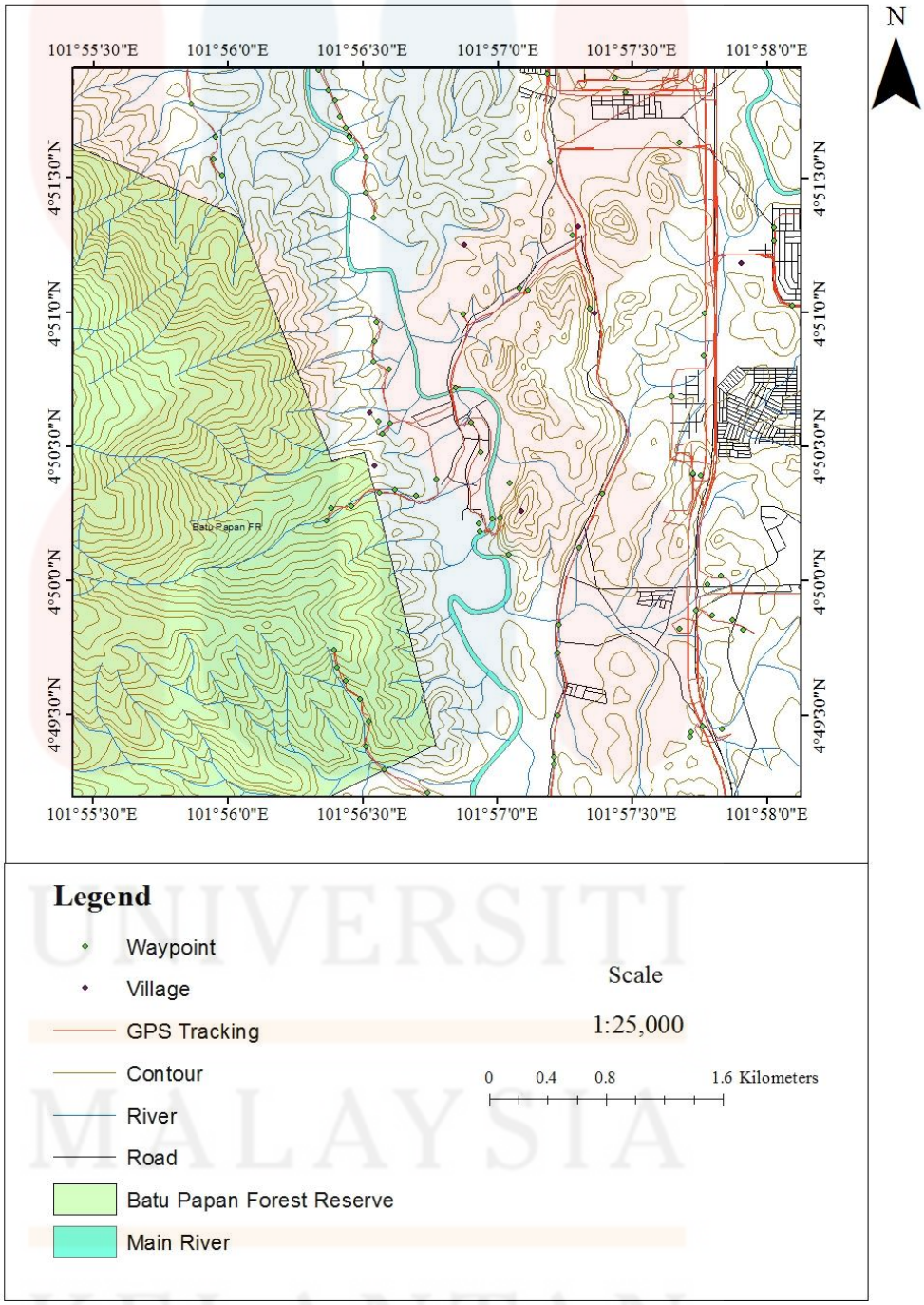


**Figure 4.2** : Traverse map

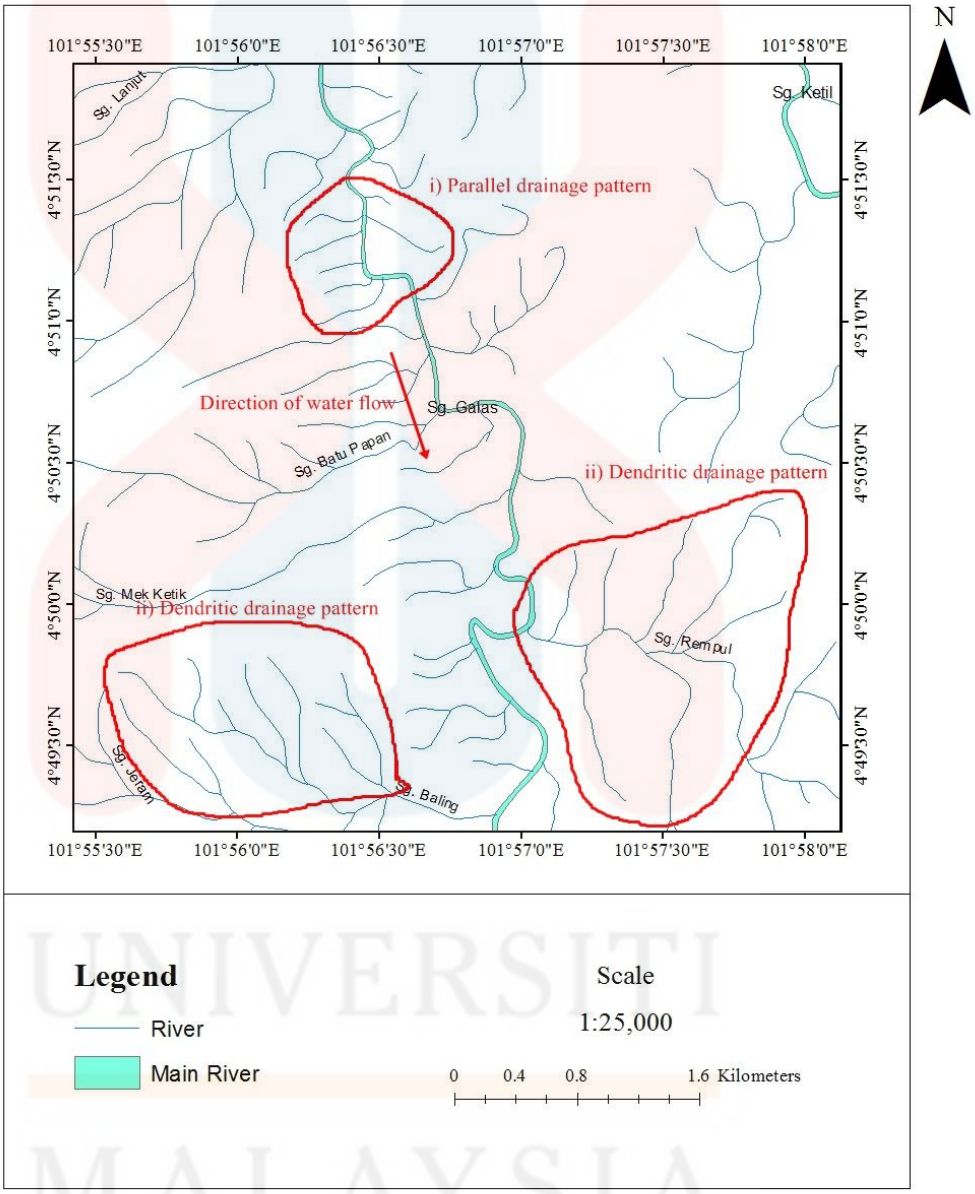


**Figure 4.3** : Drainage pattern of study area

FYP FSB
UNIVERSITI MALAYSIA KELANTAN

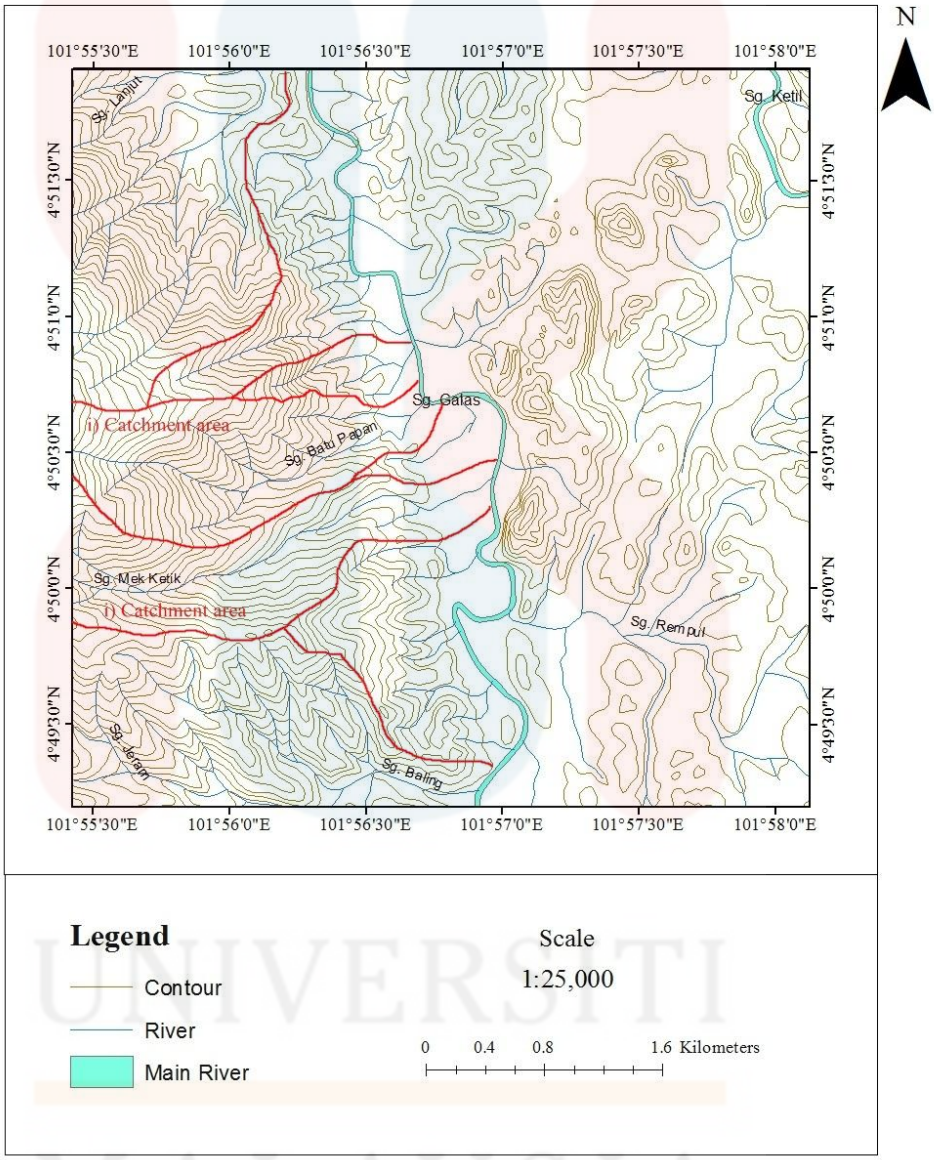


**Figure 4.4** : Drainage catchment area

FYP FSB
UNIVERSITI MALAYSIA KELANTAN

### 4.2.3 Topographic Map

A topographic map, as distinguished from other kinds, portrays by some means the shape and elevation of the terrain. Geological Survey topographic maps usually represent elevations, landforms, and the shapes into which the earth's surface is sculptured by natural forces by contour lines.

Based on topography map in Figure 4.4, the morphology of the study area can be predicted. The contour lines that form steep hills can be deduced as limestone towers. Contour groups with relatively uniform contour spacing, indicates the uniform steepness can be interpreted as igneous rock, as they are more weathering resistant and they weathered uniformly.

The elevation of the 3 D topographic map is determined by the different colours on the map. The highest elevation on the map, range between 560 – 620 m, represented by the white colours, is located at the west side. The highest elevation indicates that the top of the hills are present in this area. The lowest elevation, 80 – 140 m, represented by the blue colour, are located from the northwest to the southeast of map.

The average elevation of the map is between 80 – 140 m, represented by the blue colour, from east to the west. This indicates that most of the area has been developed for development such as roads, houses, and plantation. At Gua Madu, which is located near to centre from the east, the elevation is between 140 – 260 m, represented by the light and dark green colours, and indicates that limestone hills are present in the area. The highest elevation at Gua Madu is between 260 – 320 m, indicates the top of the hill.

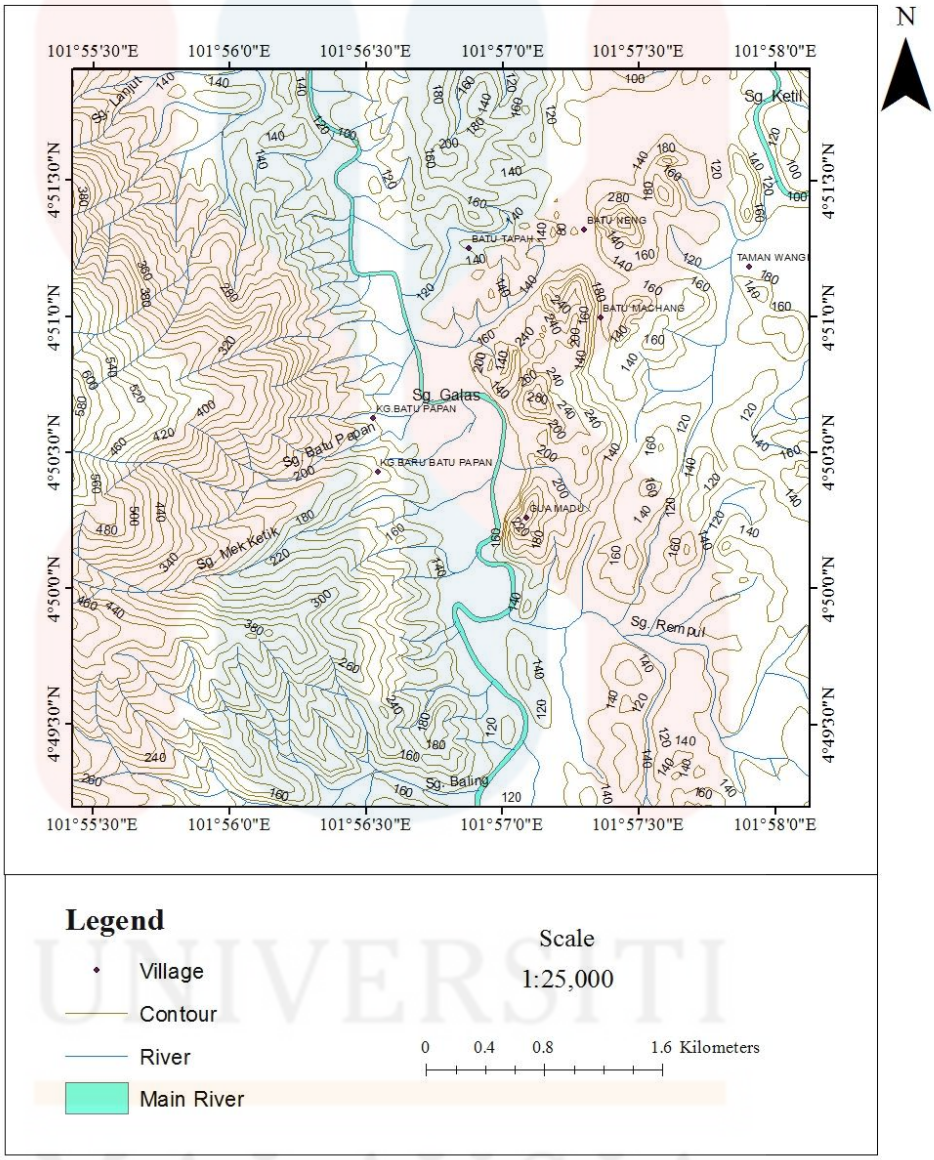


**Figure 4.5** : 2D topographic map

FYP FSB
UNIVERSITI MALAYSIA KELANTAN

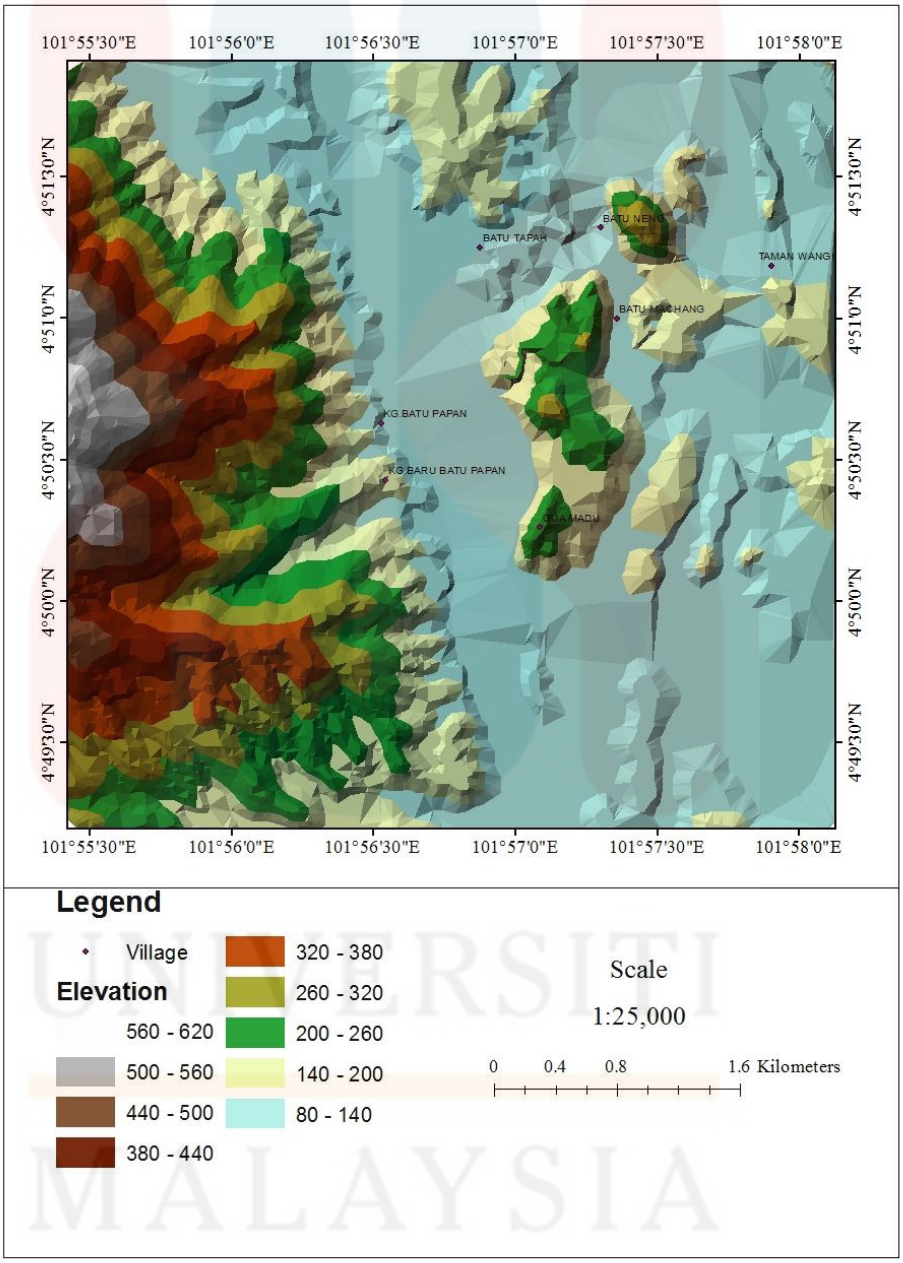


**Figure 4.6** : 3D topographic map

### 4.2.4 Weathering process

Weathering is the breaking down or dissolving of rocks and minerals on Earth surface. Water, ice, acids, salt, plants, animals, and changes in temperature are all agents of weathering. Once the rock has been broken down, a process called erosion transports the bits of rock and minerals away. No rock on Earth's surface is solid enough to resist weathering. Weathering and erosion constantly modify the Earth.

Weathering wears away exposed surfaces over time. It smooth's sharp, rough areas on rocks. Weathering also helps create soil as tiny bits of weathered rock mix with plant and animal remains. Weathering can be a physical, chemical or biological process.

a) Physical weathering

Physical weathering is caused by the effects of changing temperature on rocks, causing the rock to break apart. There are many types of physical weathering sucha as frost wedging, crystal growth, mechanical exfoliation, root penetration, thermal contraction and expansion and abrasion.

Based on Figure 4.7, the type of physical weathering is thermal contraction and expansion. The enlargement and reduction of crystal structure at Gua Madu occur in response to heating and cooling from surrounding area.

b) Chemical weathering

Chemical weathering is the breakdown of rock by chemical mechanisms. It does not break rocks into smaller fragments through wind, water and ice, instead, it changes the chemical composition of the rock, usually through carbonation, hydration, hydrolysis



FYP FSB
UNIVERSITI MALAYSIA KELANTAN

or oxidation. is caused by rain water reacting with the mineral grains in rocks to form new minerals and soluble salts. These reactions occur particularly when the water is slightly acidic.

$$CaCO_3 + CO_2 + H_2O \rightarrow Ca^{2+} + 2HCO^{3-}$$

There are different types of chemical weathering, solution, hydrolysis and oxidation. Solution is removal of rock in solution by acidic rainwater. In particular, limestone is weathered by rainwater containing dissolved CO2, and this process is sometimes called carbonation. Carbonation process happened when carbon dioxide in the air dissolves in rainwater and becomes weakly acidic. This weak "carbonic acid" is able to dissolve limestone as it seeps into cracks and cavities. Over many years, solution of the rock can form spectacular cave systems.

c) Biological weathering

Biological weathering is the weakening and subsequent disintegration of rock by plants, animals and microbes. The roots of plants cause rocks to disintegrate. Plant roots grow down through soil and rocks to find water and minerals. The roots can grow through cracks in rocks to find groundwater. As the roots grow the cracks are made wider and eventually the rock breaks up. Dead plants can cause chemical weathering. The plants produce acids when they rot.

Figure 4.6 shows the presence of biological weathering. The roots of the trees intruded through joints or cracks in the rock in order to find moisture. As the tree grows, the roots gradually prize the rock apart.



FYP FSB
UNIVERSITI MALAYSIA KELANTAN

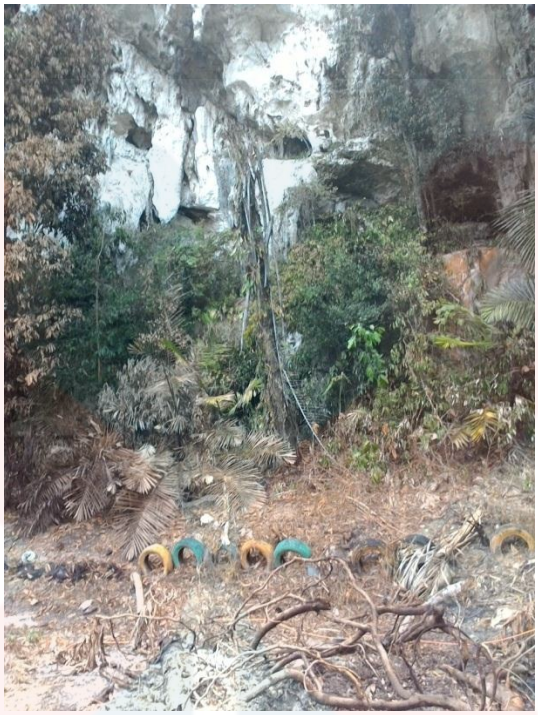

**Figure 4.7**: Effect of biological weathering that occurs at Gua Madu

**Figure 4.8** : Effect of physical weathering that can be seen near Gua Madu

### 4.2.5 Landslide

Landslide is the movement of earth material like mass of rock, debris or earth down a slope. Landslide can be defined as a massive mass of soil and rock debris that move downhill because of gravitational force. The sheer mass of material involve at the speed which they occurred make them potentially disastrous as a consequence because of the existence damage they can cause to property and lives. ( National Slope Master Plan, 2009 )

There are a few types of landslide such as rotational slumps, translational sliding, rock fall, and debris avalanche. Rotational slumps involve sliding along a curved slip plain production slumps blocks. Translational sliding is down slope movement of earth materials along a planar slip plain such as bedding plane or fracture. Rock fall is the free fall of Earth materials from a free face of a cliff. A debris avalanche is a very rapid to extremely rapid debris flow. Figure 4.8 shows the movement types and materials involves in landslide.

Based on Figure 4.9, the type of landslide is slump. The soil moved as a unit along a curved surface pull by gravitational force. In Figure 4.10 and 4.11, the type of landslide is earthflow. This is due to mass wasting events in which turbulence occurs throughout the mass. In Figure 4.12, the type of landslide is rockfall. Rockfall occur when pieces of rock break loose from a steep rock face or cliff.

FYP FSB
UNIVERSITI MALAYSIA KELANTAN

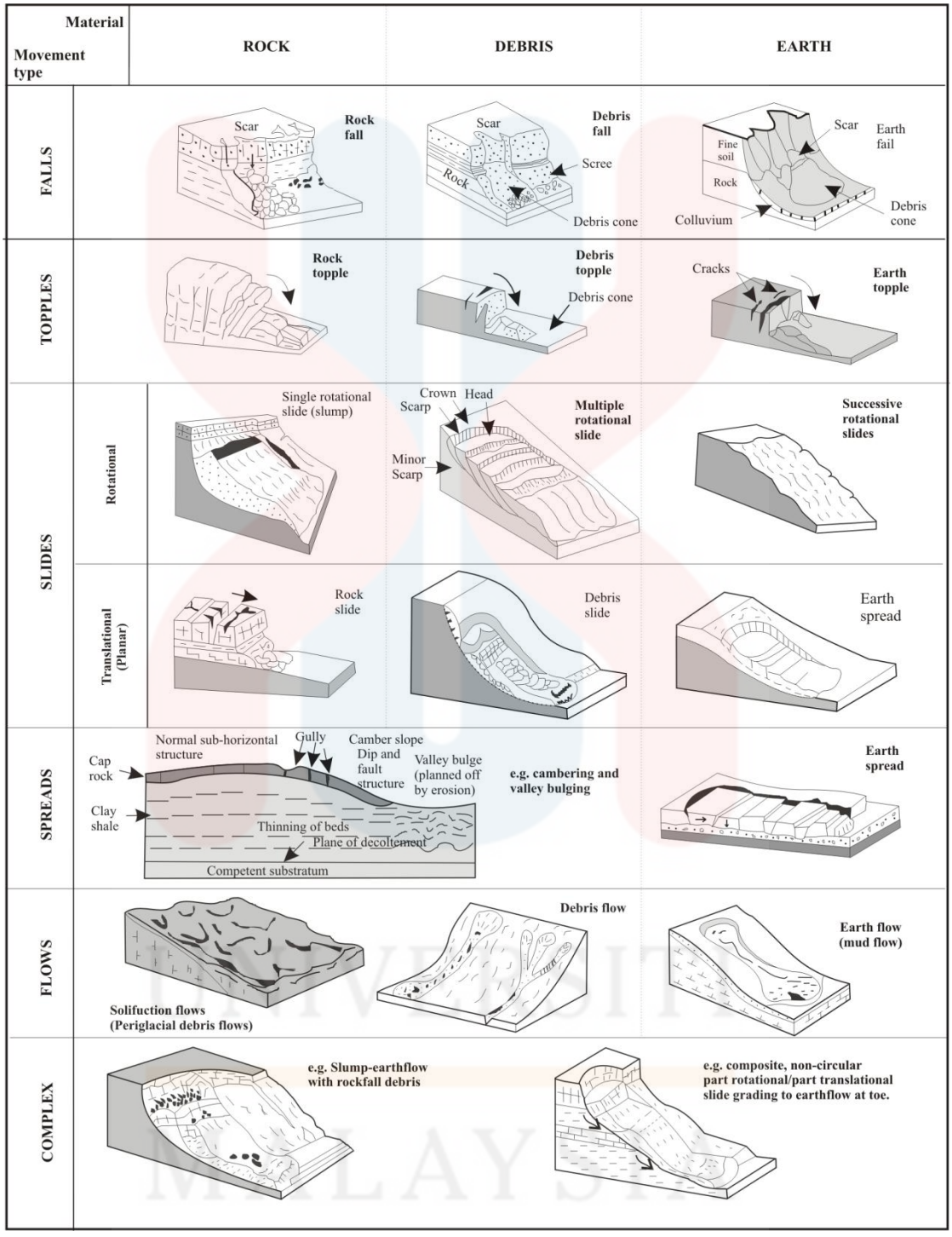


Figure 4.9 : Types of landslide (Slope Failure Classification by British Geological Survey, 1999)

**Figure 4.10** : Slump at Kampung Batu Papan

**Figure 4.11** : Earthflow near Perhentian Gua Musang

**Figure 4.12** : Earthflow at Taman Wangi

**Figure 4.13** : Rock fall near the main road to Kampung Batu Papan

## 4.3 Petrography

Petrography is the branch of geology that focuses on the detailed description of minerals in rocks, by using microscope. Five rock samples are taken during geological mapping to study about the rocks and minerals of the study area.

For carbonate sedimentary rock, Folk and Dunham classification is used. Folk's classification is based on the relative abundance of three elements of carbonate rocks. The examples are: carbonate grains ( allochem ), lime mud ( micrite ), and sparry calcite cement. Dunham's classification, on other hand, is focusing on rock depositional textures features which is grain packing, ratio of allochem to micrite, and grain binding ( Ford, 1962). Table 4.1 and Figure 4.11 show the classification of Folk and Dunham class.

For igneous rock, International Union of Geological Sciences ( IUGS ) systematics is used. The work of Le Bas and Strecksein in 1991 for IUGS produced among others, QAPF classification for plutonic and volcanic rocks. The QAPF classification works based on ratio of quartz (Q), alkali feldspar (A) and plagioclase (P), plagioclase (P) and feldspathoids (F). Figure 4.12 shows QAPF diagram which classifies and guides naming of plutonic igneous rocks.

FYP FSB
UNIVERSITI
MALAYSIA
KELANTAN

| Allochthonous limestone original components not organically bound during deposition | | | | | | Autochthonous limestone original components organically bound during deposition | | |
|---|---|---|---|---|---|---|---|---|
| Less than 10% >2 mm components | | | | Greater than 10% >2 mm components | | Boundstone | | |
| Contains lime mud (<0.02 mm) | | | No lime mud | Matrix supported | >2 mm component supported | By organisms which act as barriers | By organisms which encrust and bind | By organisms which build a rigid framework |
| Mud supported | | Grain supported | | | | | | |
| Less than 10% grains (>0.02 mm to <2 mm) | Greater than 10% grains | | | | | | | |
| Mudstone | Wackestone | Packstone | Grainstone | Floatstone | Rudstone | Bafflestone | Bindstone | Framestone |

**Table 4.1** : Dunham's classification ( from Kendall 2005 )

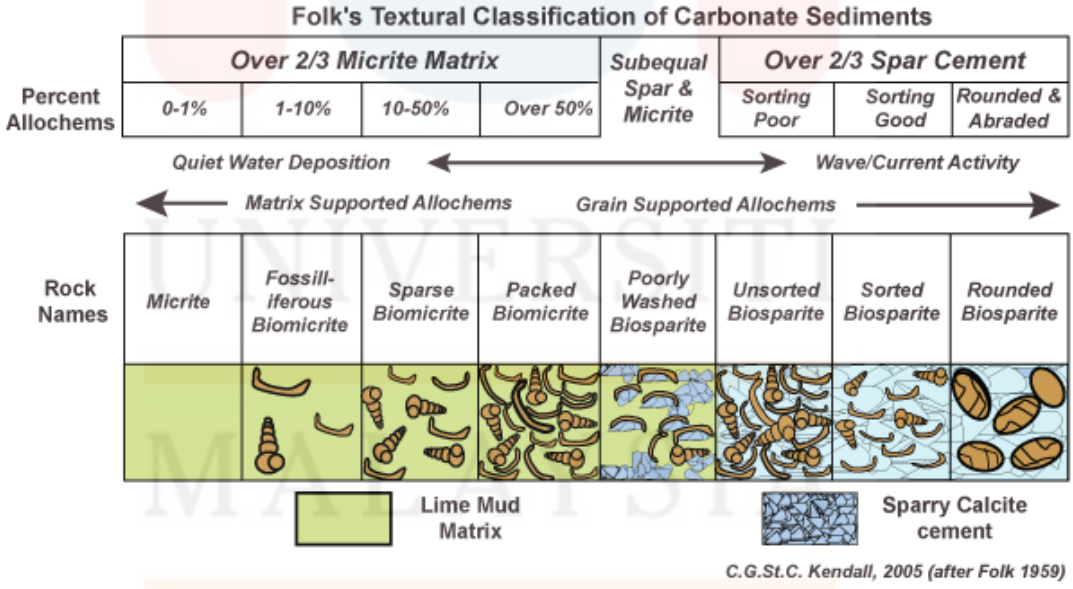


**Figure 4.14** : Folk's classification ( from Kendall 2005 )

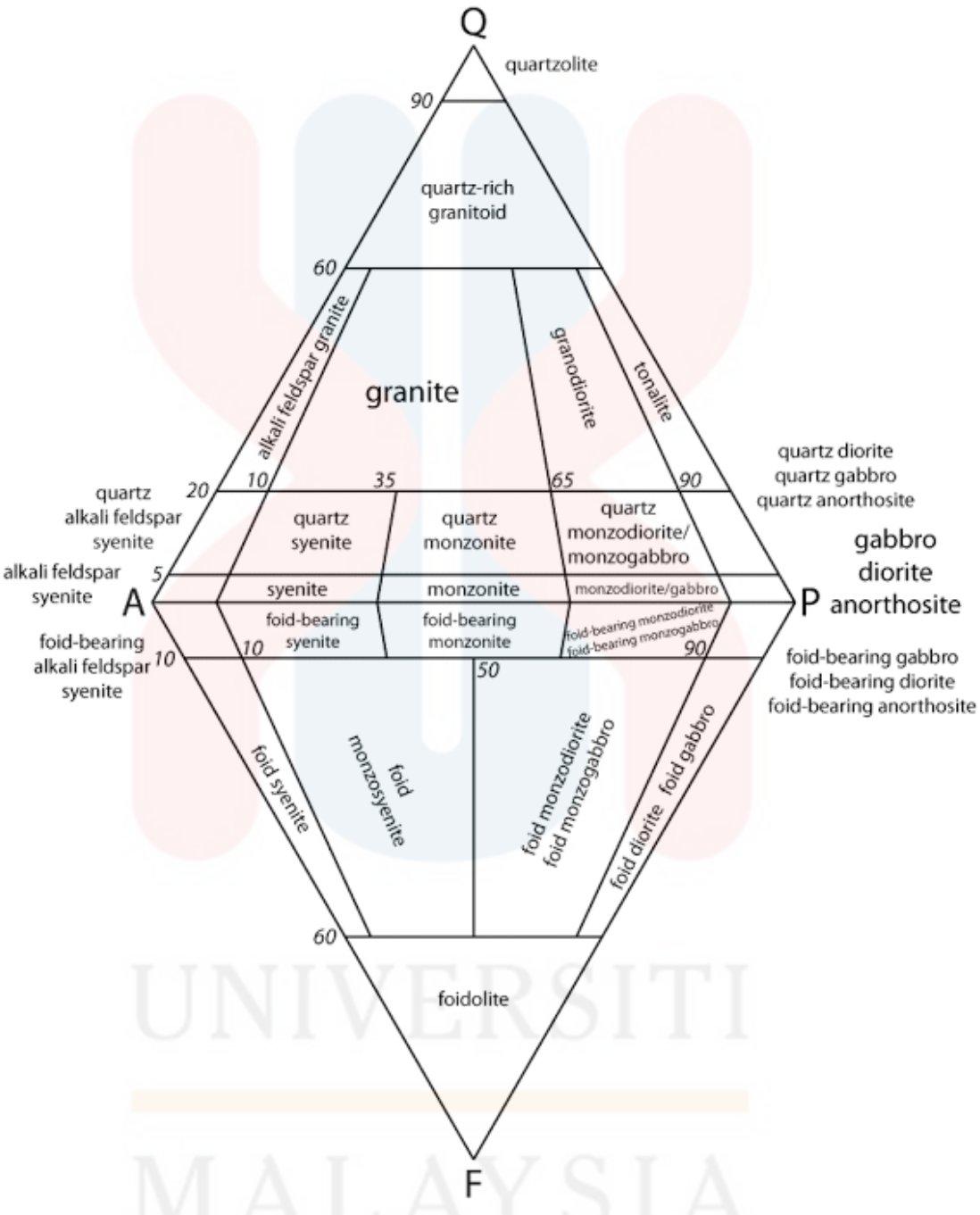


**Figure 4.15** : QAPF diagram for classification and nomenclature of plutonic igneous rocks ( Le Bas & Strecksein,1991 )

FYP FSB
UNIVERSITI MALAYSIA KELANTAN

### 4.3.1 Study Area

Seven rock samples are taken during geological mapping at the study area.The study area is mostly dominated by the two type of rocks which is sedimentary and igneous rock. Limestone and sandstone are sedimentary rocks while granite and tuff are igneous rock. In Figure shows the location of each outcrop.

Sample 1

Coordinate : N 4° 51’ 0.55” E 101° 57’ 7.36”

Location : Rockfall area, Kg Batu Papan

a) Tuff

Tuff is an igneous rock that forms from the products of an explosive volcanic eruption. In these eruptions, the volcano blasts rock, ash, magma and other materials from its vent. This cause the rock to travels through air and falls back to Earth in the area surrounding the volcano.

Tuff is usually thickest near the volcanic vent and decreases in thickness with distance from the volcano. Some tuff deposits are hundreds of meters thick and have a total eruptive volume. That enormous thickness can be from a single eruptive blast, or from successive surges of a single eruption. It also can come from eruptions that were separated by long periods of time. Figure 4.17 shows the location of outcrop at station 1 while Figure 4.18 shows the hand specimen of outcrop

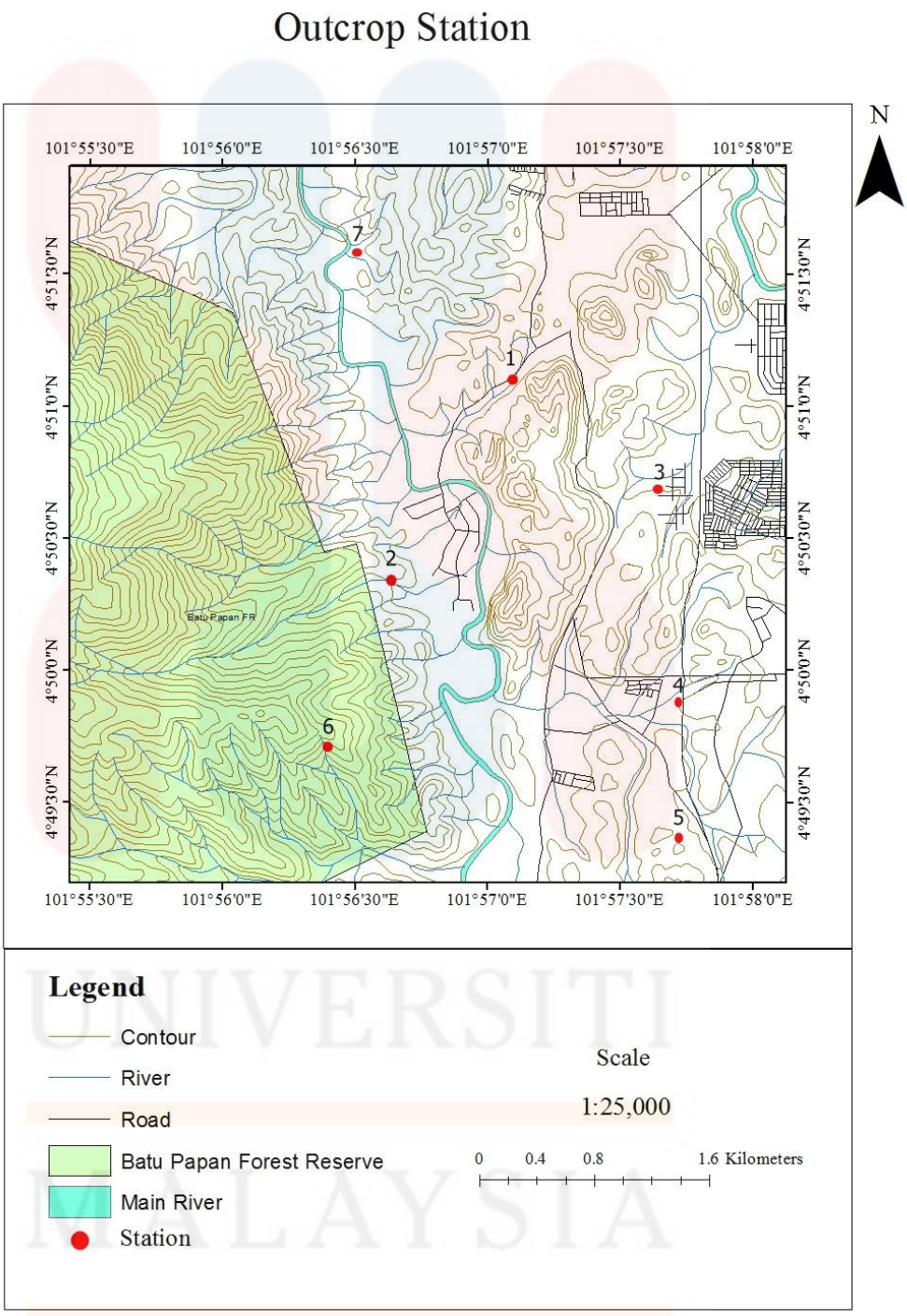


**Figure 4.16** : Outcrop Station for each sample

FYP FSB
UNIVERSITI MALAYSIA KELANTAN

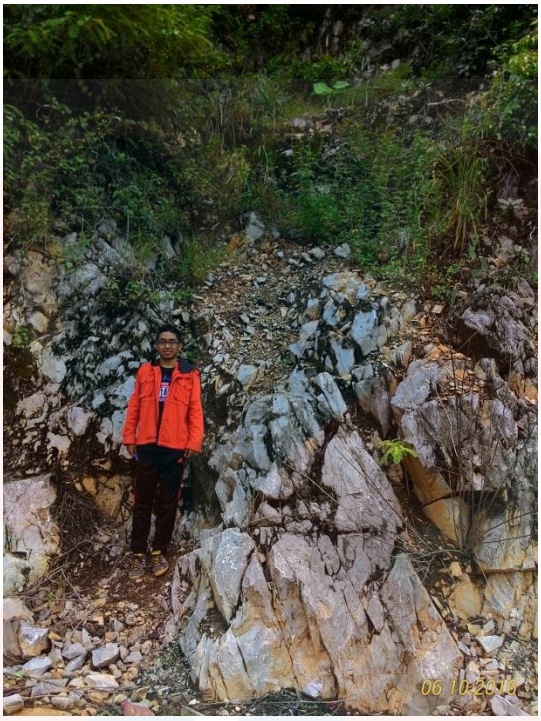


**Figure 4.17** : Location of outcrop at station 1

**Figure 4.18** : Hand specimen of outcrop at station 1

Thin Section Sample 1

Plane polarized

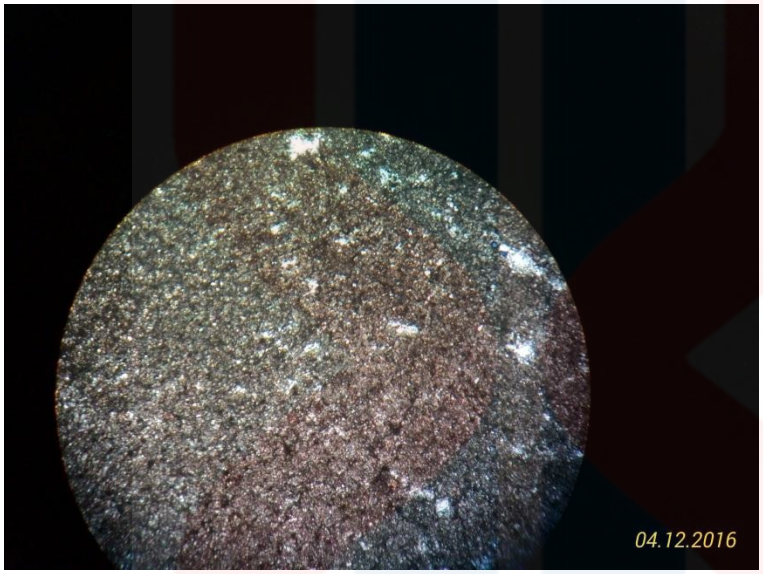

(4x)

Cross polarized

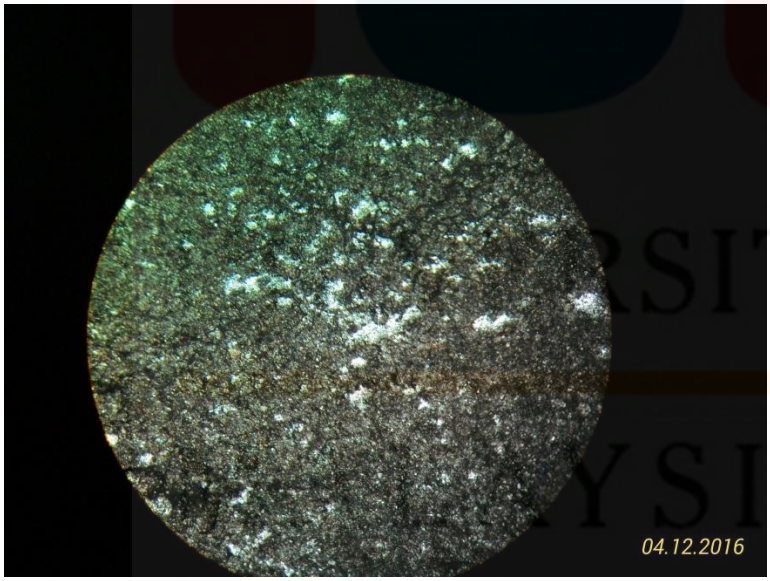

(4x)

Pumice : 10%

Crystal fragments : 20%

Rock fragments : 70 %

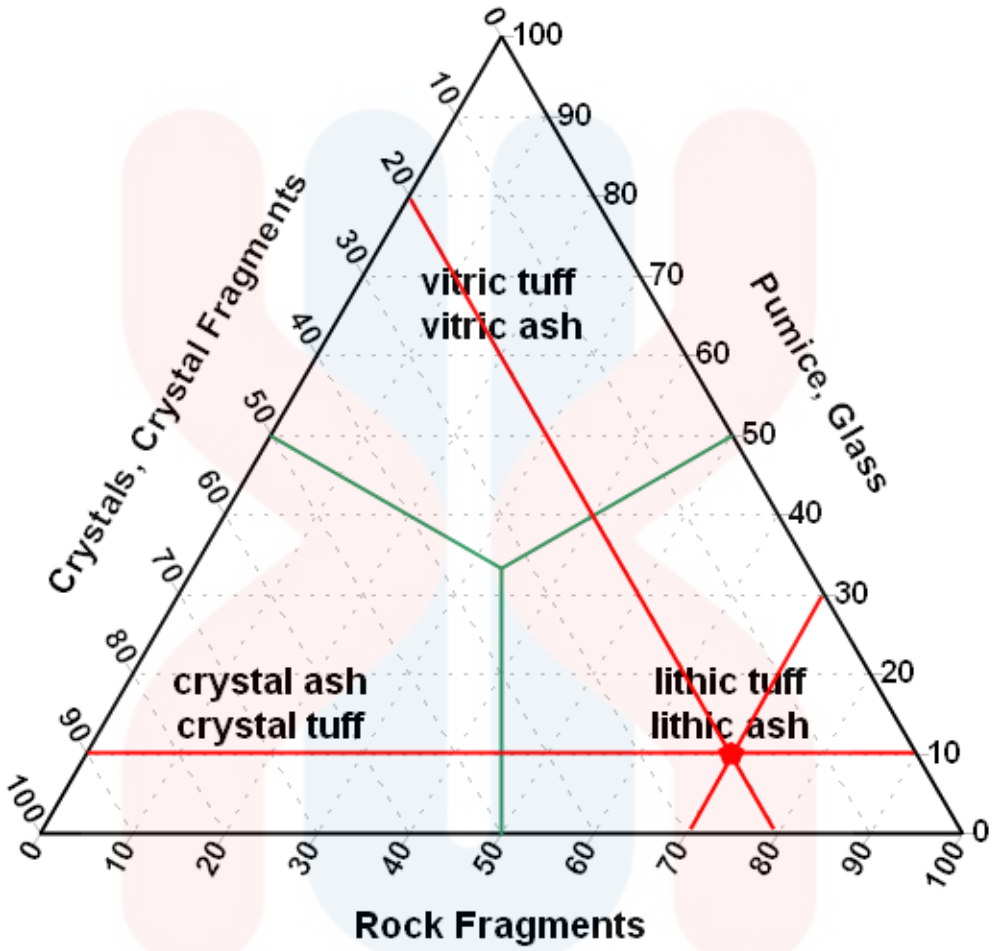


Name of the rock : Lithic tuff

FYP FSB
UNIVERSITI
MALAYSIA
KELANTAN

Sample 2

Coordinate : N 4° 50’ 21.23’’ E 101° 56’ 38.46’’

Location : Near river in Kg Batu Papan

b) Limestone

Limestone is a sedimentary rock composed primarily of calcium carbonate ( $CaCO_3$) in the form of mineral calcite. It most commonly forms in clear, warm, shallow marine waters. It is usually an organic sedimentary rock that forms from the accumulation of shell, coral, algal, and facial debris. It can be also be a chemical sedimentary rock formed by the precipitation of calcium carbonate from lake or ocean water.

Limestone, by definition is a rock that contains at least 50% calcium carbonate in the form of calcite by weight. All limestone contains at least a few per cent of quartz, feldspar, clay minerals, pyrite, and other minerals.

Figure 4.19, 4.21 and 4.25 shows the location of outcrop as station 2, 3 and 5 while in Figure 4.20, 4.22 and 4.26 shows the hand specimen of each location.

FYP FSB
UNIVERSITI MALAYSIA KELANTAN

**Figure 4.19** : Location of outcrop at station 2

**Figure 4.20** : Hand specimen of outcrop at station 2

FYP FSB
UNIVERSITI MALAYSIA KELANTAN

Thin Section Sample 2

Plane-polarized

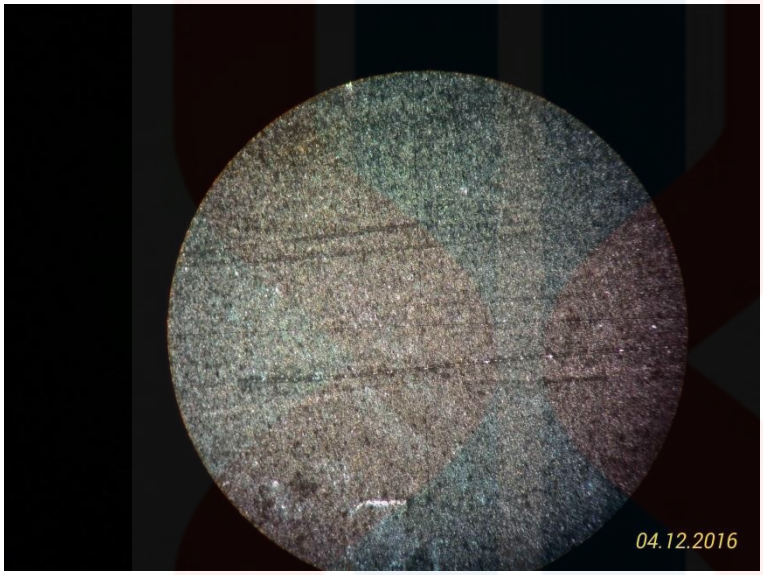

(4x)

Cross-polarized

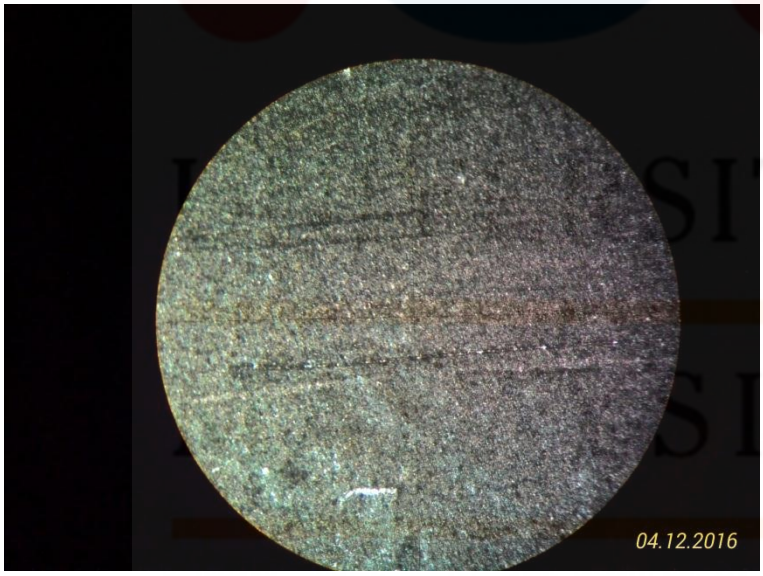

(4x)

FYP FSB

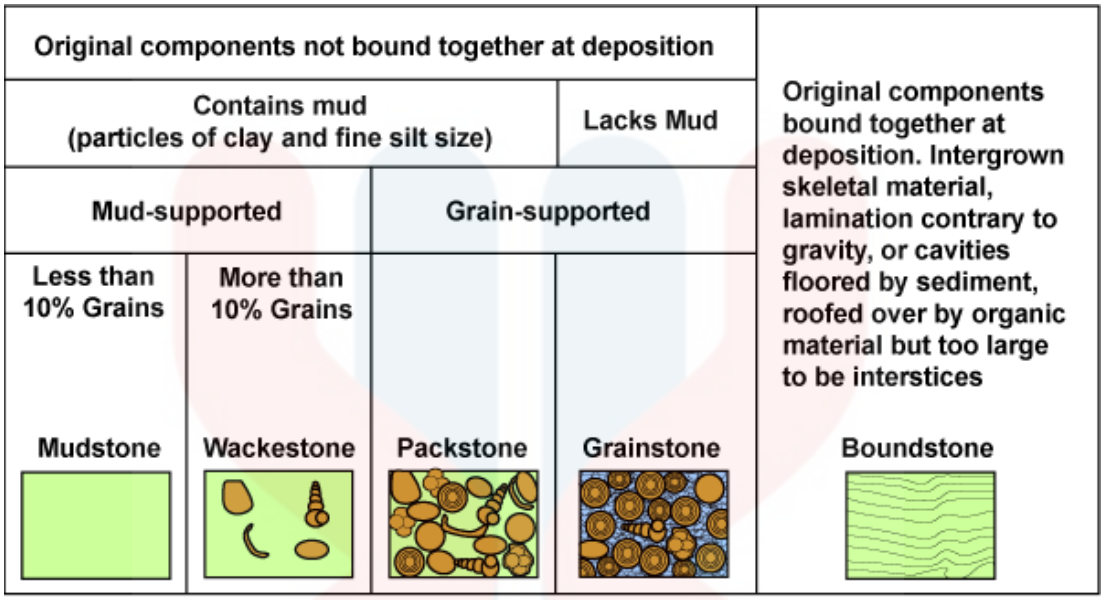


*C. G. St. C. Kendall, 2005 (after Dunham, 1962, AAPG Memoir 1)*

Based on Dunham's classification,

1. Original components not bound together at deposition

2. Contains mud

3. Less than 10% grains

Name of the rock : Lime mudstone

FYP FSB
UNIVERSITI MALAYSIA KELANTAN

Sample 3

Coordinate : N 4°50’ 43.21’’ E 101° 57’ 57.25’’

Location : At the construction site near main road to Kg Batu Papan

**Figure 4.21** : Location of outcrop at station 3

**Figure 4.22** : Hand specimen of outcrop at station 3

Thin Section Sample 3

Plane-polarized

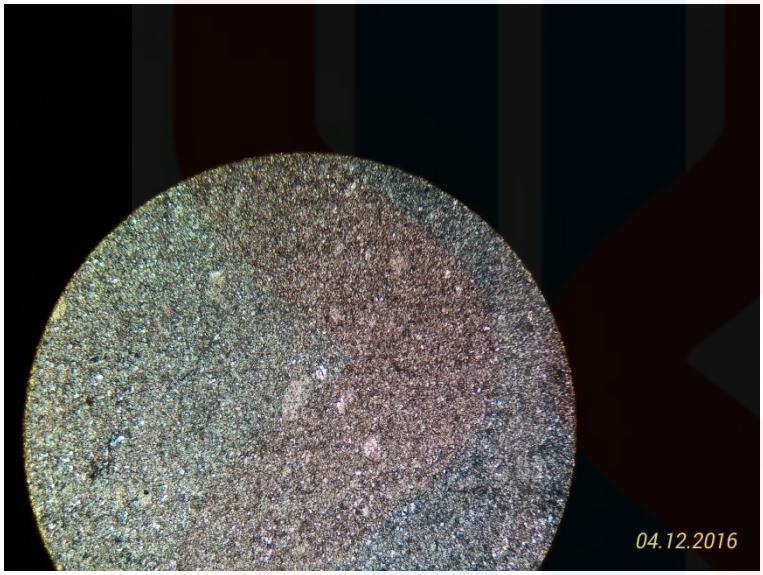

(4x)

Cross-polarize

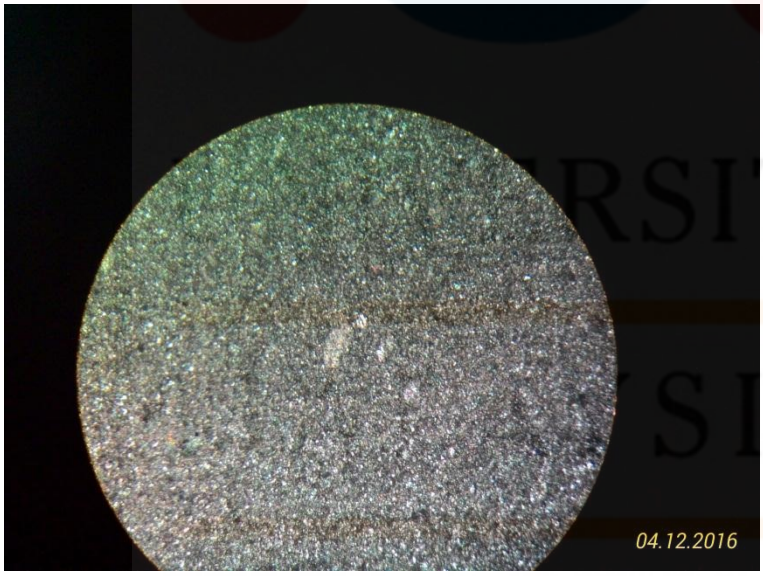

(4x)

FYP FSB
KELANTAN

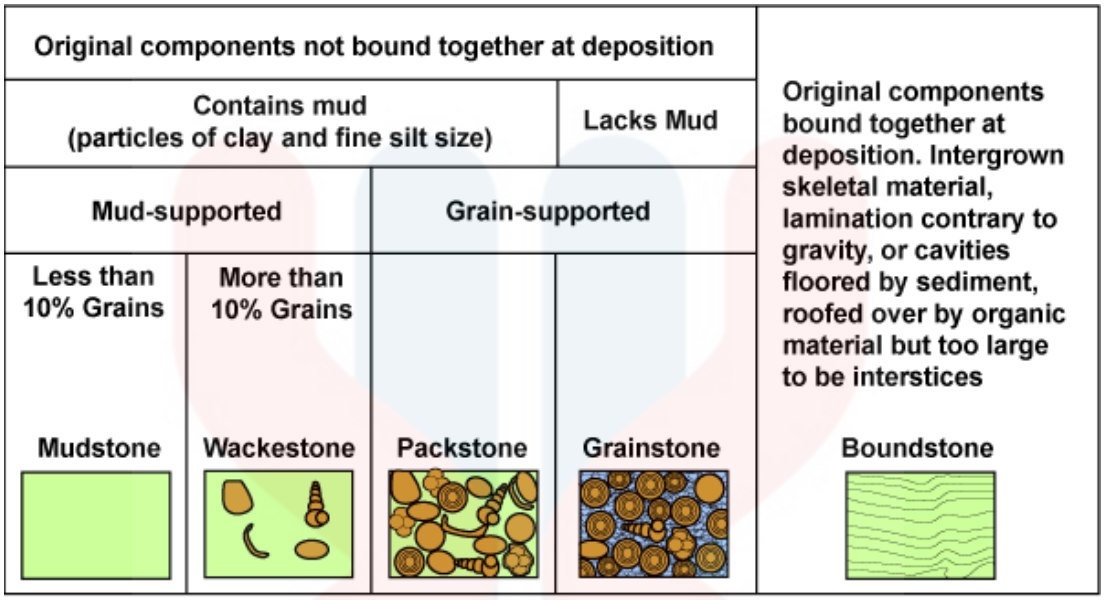


*C. G. St. C. Kendall, 2005 (after Dunham, 1962, AAPG Memoir 1)*

Based on Dunham's classification,

1. Original components not bound together at composition

2. Contains mud

3. Less than 10% grains

Name of the rock : Lime mudstone

FYP FSB
UNIVERSITI
MALAYSIA
KELANTAN

Sample 4

Coordinate : N 4° 49’ 53.48’’ E 101° 57’ 44.47’’

Location : Roadside near residential area at Taman Wangi

c) Granite

Granite is a light-coloured igneous rock with grains large enough to be visible with the unaided eye. It forms from the slow crystallization of magma below Earth’s surface. Granite is composed mainly of quartz and feldspar with the minor amounts of mica, amphiboles and other minerals. This mineral composition usually gives granite a grey or white colour with dark mineral grains visible throughout the rock.

Granite is a plutonic rock in which quartz makes up between 10 and 50 percent of the felsic components and alkali feldspar for about 65 to 90 percent of the total feldspar content.

FYP FSB
UNIVERSITI
MALAYSIA
KELANTAN

**Figure 4.23** : Location of outcrop at station 4

**Figure 4.24** : Hand specimen of outcrop at station 4

Thin Section Sample 4

Plane-polarize

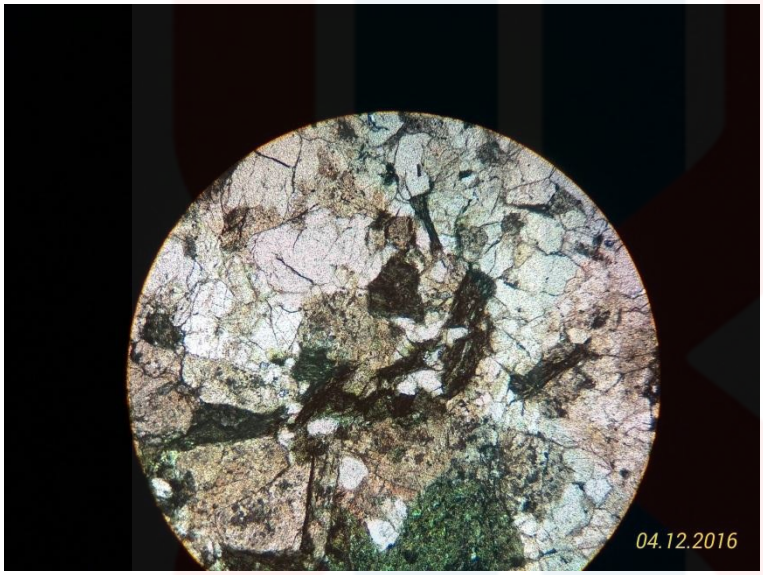

(4x)

Cross-polarize

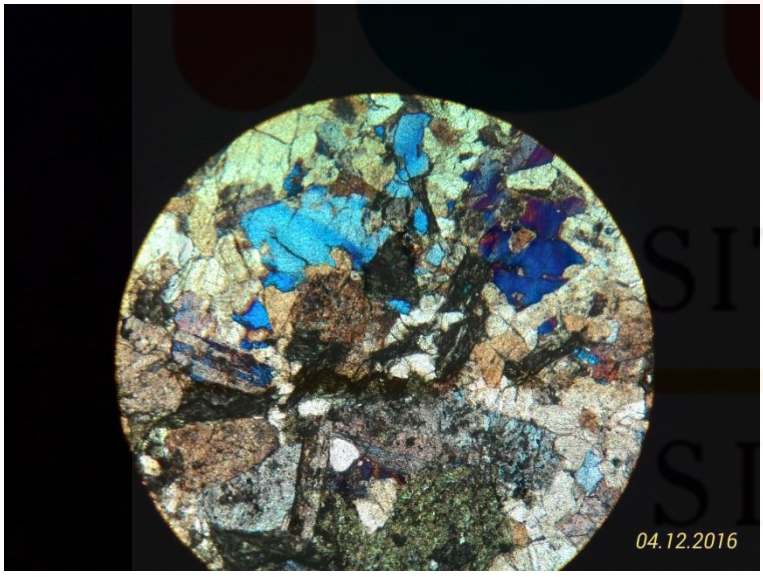

(4x)

Quartz : 40%

Alkali feldspar : 40%

Plagioclase : 20%

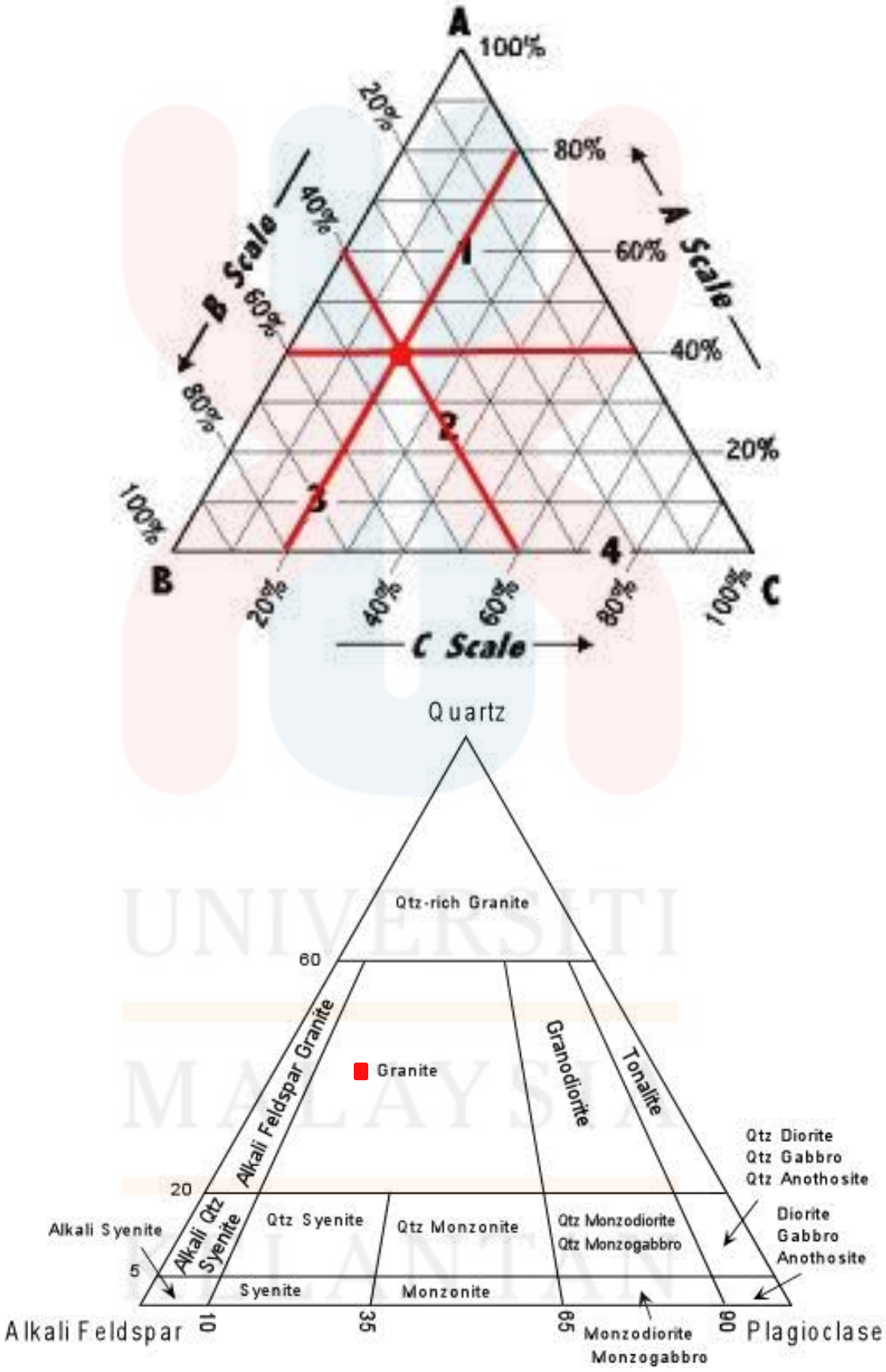


Name of the rock : Granite

Sample 5

Coordinate : N 4° 49’ 20.55’’ E 101° 57’42.62’’

Location : At landslide area near Hentian Gua Musang

**Figure 4.25** : Location of outcrop at station 5

FYP FSB
UNIVERSITI
MALAYSIA
KELANTAN

**Figure 4.26** : Hand specimen of outcrop at station 5

FYP FSB
UNIVERSITI
MALAYSIA
KELANTAN

Thin Section Sample 5

Plane-polarize

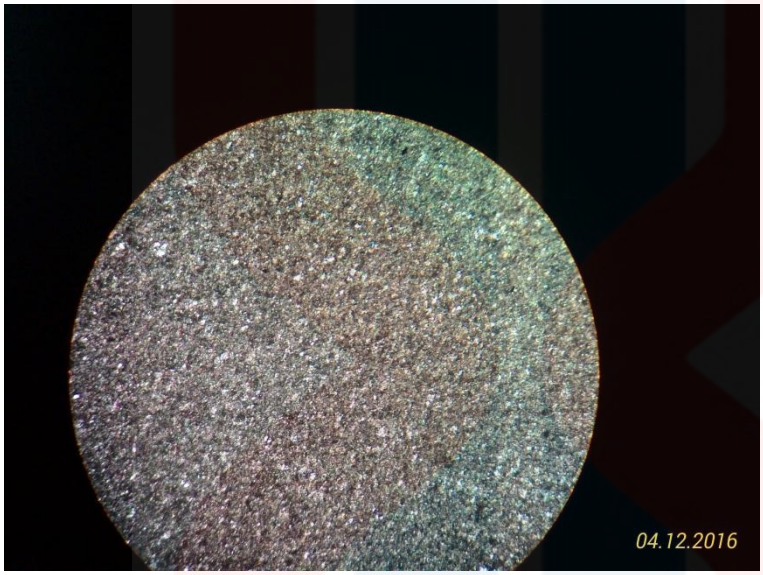

(4x)

Cross polarized

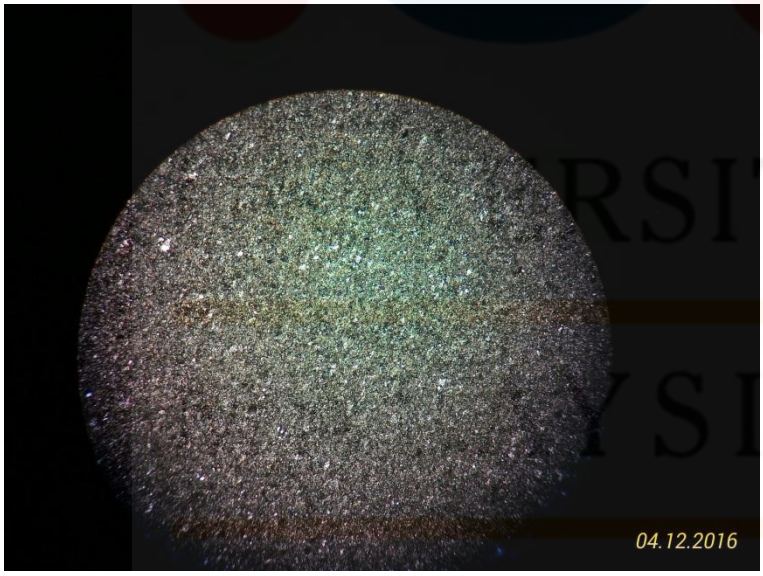

(4x)

FYP FSB
UNIVERSITI MALAYSIA KELANTAN

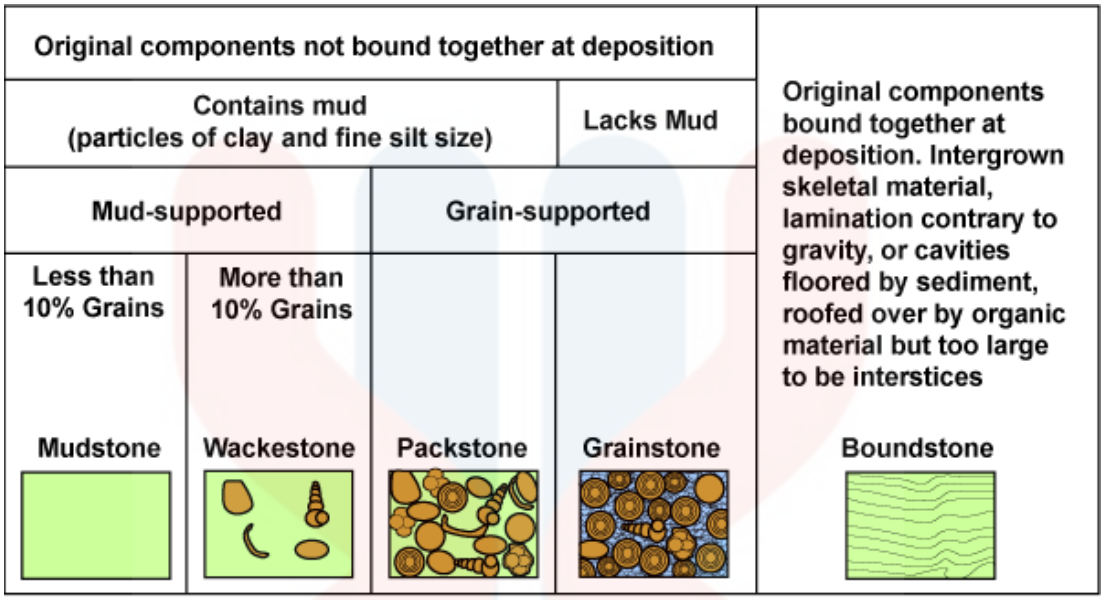


*C. G. St. C. Kendall, 2005 (after Dunham, 1962, AAPG Memoir 1)*

Based on Dunham's classification,

1. Original components not bound together at composition

2. Contains mud

3. Less than 10% grains

Name of the rock : Lime mudstone

FYP FSB
UNIVERSITI
MALAYSIA
KELANTAN

Geological Map of Study Area

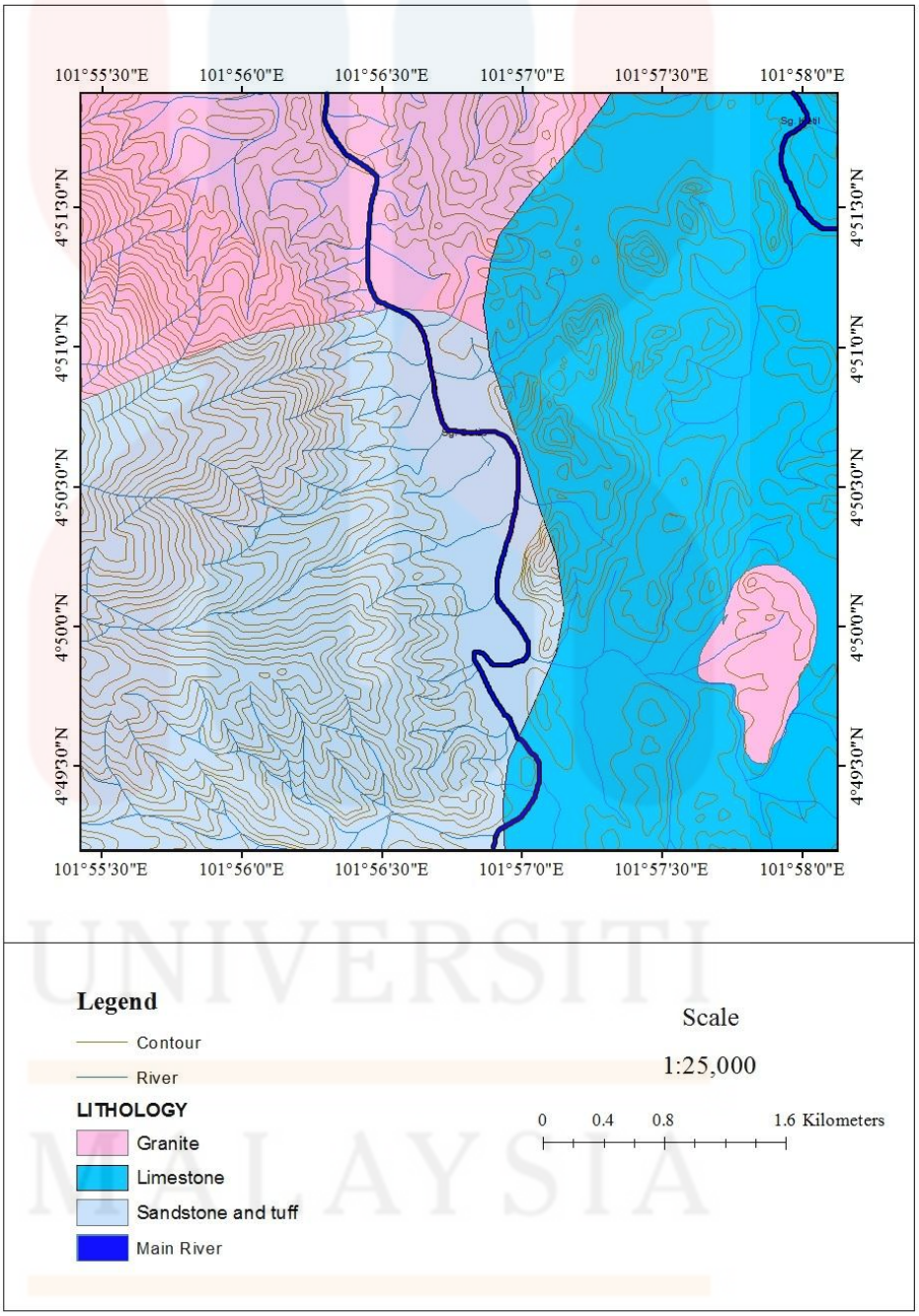


## 4.4 Stratigraphy

Stratigraphy is the study of stratified rocks in terms of time and space. It deals with the correlation of rocks from different localities. The correlation can be made by using biostratigraphy method which use fossils as an indicator and lithostratigraphy method which use the geological time units.

Each of the rock has their specific age. The age is measure by using geological time scale. The oldest rock in the study area is from the Permian period in Palaeozoic era which is limestone. Sandstone also is from the Palaeozoic era in the Permian period. The youngest rock is granite because it is acid intrusive and formed in Tertiary period during Cenozoic era.

| ERA | PERIOD | TYPE OF ROCKS |
|---|---|---|
| Mesozoic | Triassic | Granite |
| Palaeozoic | Permian | Sandstone and tuff |
| | | Limestone |

**Table 4.2** : Stratigraphic column of study area

FYP FSB
UNIVERSITI MALAYSIA KELANTAN

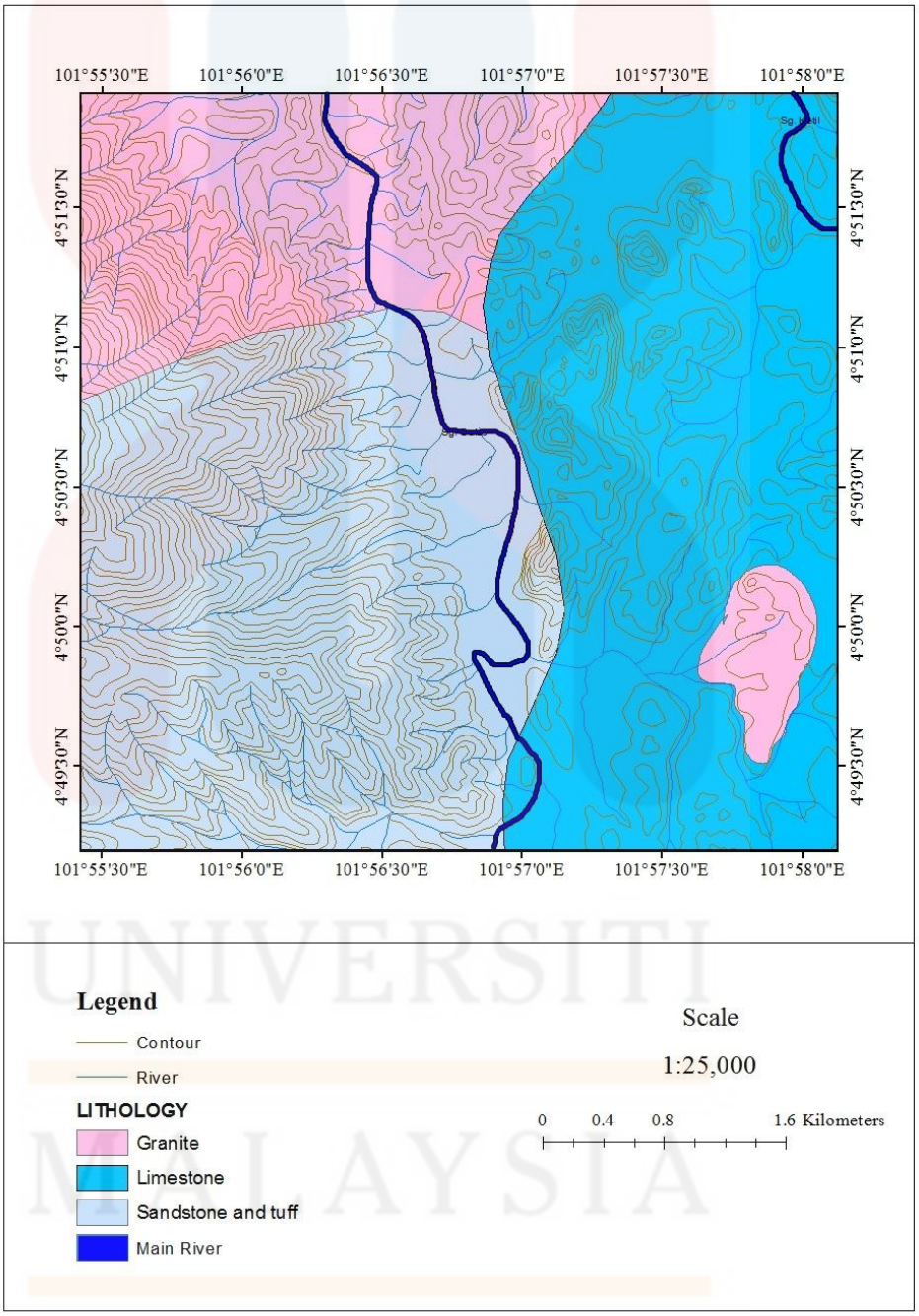


**Figure 4.27** : Geological map of study area

FYP FSB
UNIVERSITI
MALAYSIA
KELANTAN

## 4.5 Structural Geology

Structural geology is the study of the structure of the rocks at all scales and the processes that produce all of those structures. There are presents of faults in the study area. It is believes that the faults are connected to the Lebir Fault Zone that is located in the eastern part of Kelantan state, which is one of the major lineaments in Peninsular Malaysia and considered to be post-Cretaceous and sinistral strike-slip fault (Tjia, 1989 and Harun, 2002).

### 4.5.1 Lineament Analysis

Lineaments are mappable linear surface features which differ clearly from the patterns of adjacent features and presumably reflect subsurface phenomena (O'Leary et al. 1976). They are generally displayed by topography (including straight stream segments), vegetation, or soil tonal alignments (Lattman and Parizek, 1964).

Lineament analysis is a linear feature on the earth surface, such as fault. It is a straight linear structure where it was controlled by structure such as ridge, joint, fault, inconsistency and the boundary of rock. This lineament analysis is conduct by referring to the terrain map of the study area ( Figure 4.28 ). A rose diagram is produce from the data collected from the terrain map in order to know the force direction in the study area.

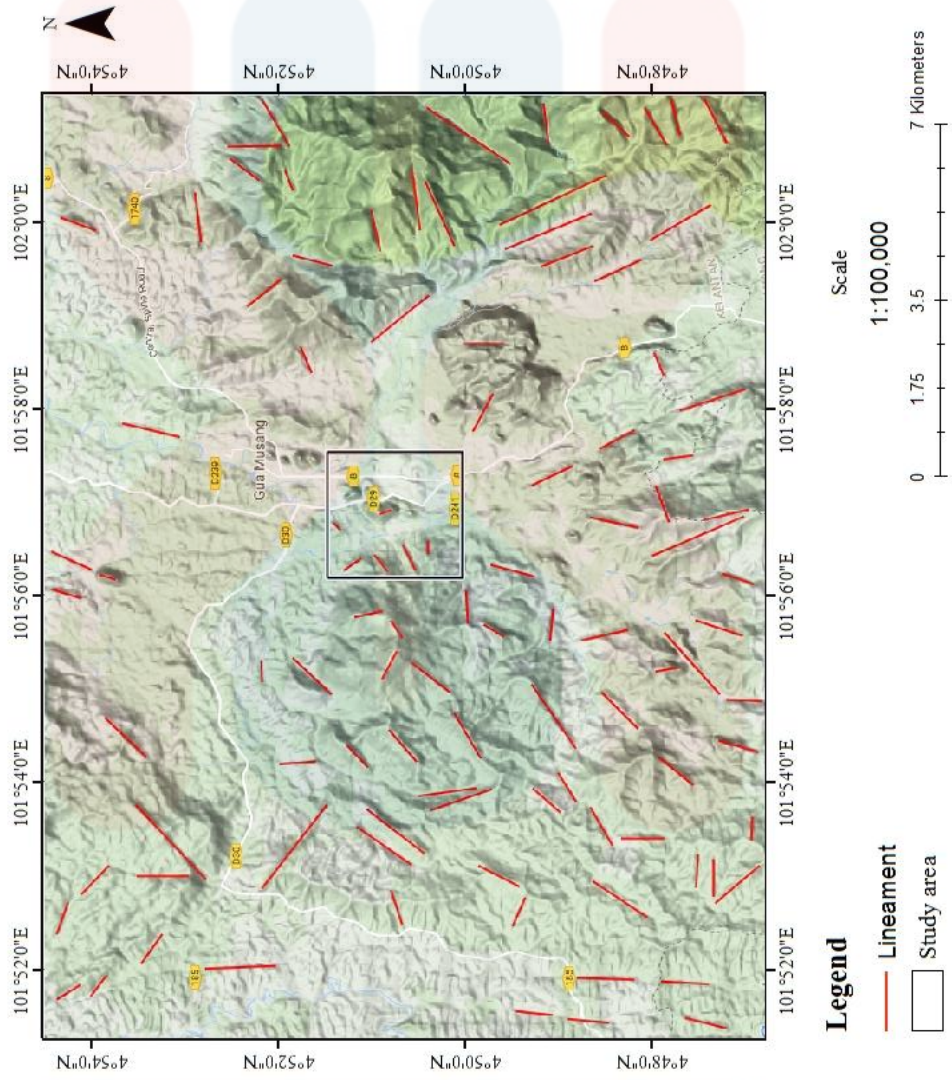


**Figure 4.28** : Lineament of study area

FYP FSB
MALAYSIA
KELANTAN

**Figure 4.29** : Rose diagram of lineament reading

Based on Figure 4.29, there are two forces that act on the rose diagram. From ES and NW, the compression forces act on the highest reading at 165° and 350° respectively. This resulting in the external forces on NE at 80° and WS at 260° based on 90° angle from the compression force.

### 4.5.2 Joint analysis

Joint is a fracture in rocks along which no visible movement has occurred. Nearly vertical joints that result from reduction during cooling are commonly found in igneous rocks. Similar joints occur in thick beds of sandstone and gneiss, with the sheets similar to the structure of a sliced onion. Deep-seated igneous rocks often have joints almost parallel to the surface, signifying that they formed by expansion of the rock mass as overlying rocks were eroded away.

Some joints in sedimentary rocks may have formed as the outcome of contraction during compaction and drying of the sediment. In some cases, jointing of the rock may result from the exploit of the same forces that cause folds and faults. In relatively uninterrupted sedimentary rocks, such joints are often in two vertical sets perpendicular to one another. Normally, streams develop along zones of weakness caused by joints in rocks, and thus the regional pattern of joint orientation often applies a strong control on the development of drainage patterns.

Joint analysis is conducted to see if there is a correlation between the joint patterns of the study area. The location of where the joint reading taken is marked on the map (Figure 4.30). For every location, the reading is taken, then is used to plot the rose diagram.

FYP FSB
UNIVERSITI MALAYSIA KELANTAN

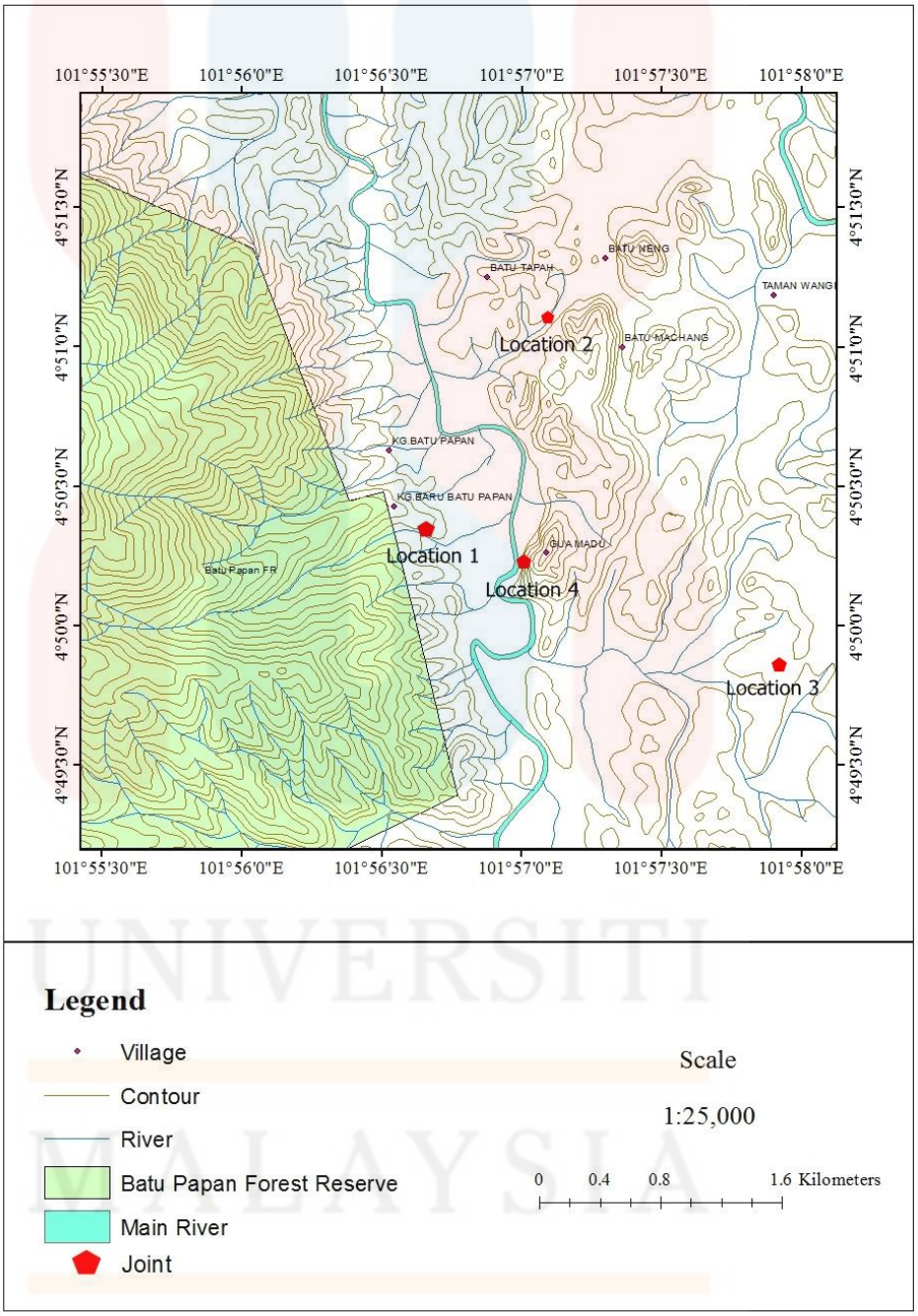


**Figure 4.30** : Joint sampling map

FYP FSB
UNIVERSITI
MALAYSIA
KELANTAN

**Table 4.3 : Joint sampling reading (location 1)**

| | | | | | | | | | |
|---|---|---|---|---|---|---|---|---|---|
| **1** | 200° | **21** | 140° | **41** | 146° | **61** | 140° | **81** | 112° |
| **2** | 140° | **22** | 120° | **42** | 102° | **62** | 166° | **82** | 152° |
| **3** | 144° | **23** | 209° | **43** | 322° | **63** | 150° | **83** | 154° |
| **4** | 100° | **24** | 122° | **44** | 300° | **64** | 62° | **84** | 124° |
| **5** | 132° | **25** | 134° | **45** | 270° | **65** | 102° | **85** | 264° |
| **6** | 141° | **26** | 126° | **46** | 278° | **66** | 144° | **86** | 139° |
| **7** | 112° | **27** | 154° | **47** | 264° | **67** | 142° | **87** | 151° |
| **8** | 139° | **28** | 108° | **48** | 268° | **68** | 209° | **88** | 108° |
| **9** | 119° | **29** | 182° | **49** | 350° | **69** | 104° | **89** | 144° |
| **10** | 120° | **30** | 210° | **50** | 316° | **70** | 322° | **90** | 268° |
| **11** | 138° | **31** | 62° | **51** | 200° | **71** | 132° | **91** | 119° |
| **12** | 166° | **32** | 104° | **52** | 138° | **72** | 92° | **92** | 160° |
| **13** | 142° | **33** | 100° | **53** | 149° | **73** | 134° | **93** | 152° |
| **14** | 141° | **34** | 112° | **54** | 210° | **74** | 112° | **94** | 316° |
| **15** | 92° | **35** | 110° | **55** | 146° | **75** | 270° | **95** | 120° |
| **16** | 118° | **36** | 124° | **56** | 140° | **76** | 141° | **96** | 156° |
| **17** | 152° | **37** | 144° | **57** | 166° | **77** | 118° | **97** | 220° |
| **18** | 151° | **38** | 152° | **58** | 150° | **78** | 126° | **98** | 158° |
| **19** | 160° | **39** | 158° | **59** | 62° | **79** | 110° | **99** | 352° |
| **20** | 156° | **40** | 220° | **60** | 102° | **80** | 278° | **100** | 100° |

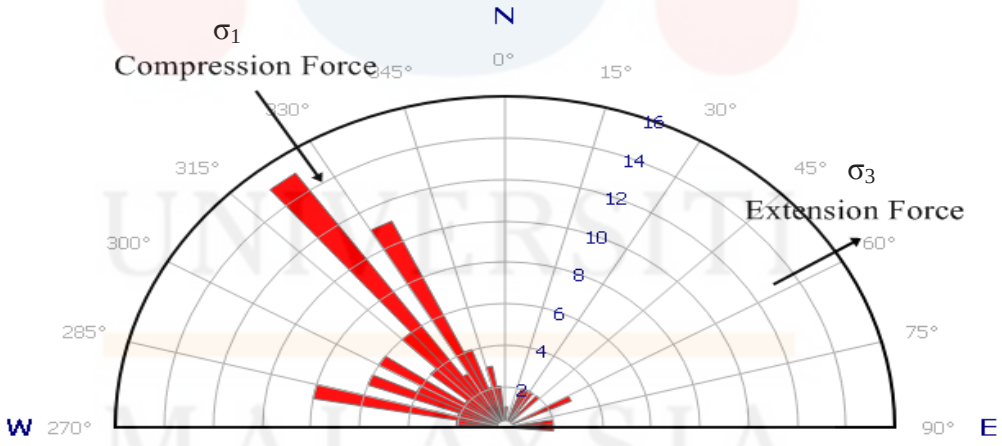


**Figure 4.31** : Rose diagram of location 1

Figure 4.31 shows that there two forces act on the joint. From NW is the compression force, based on the average of two highest reading at 220° and to NE is extension force at 55°, based on 90° angle from the compression force.

**Table 4.5 : Joint sampling reading (location 2)**

| | | | | | | | | | |
|---|---|---|---|---|---|---|---|---|---|
| **1** | 180° | **21** | 144° | **41** | 280° | **61** | 169° | **81** | 200° |
| **2** | 179° | **22** | 119° | **42** | 264° | **62** | 128° | **82** | 136° |
| **3** | 220° | **23** | 128° | **43** | 236° | **63** | 112° | **83** | 98° |
| **4** | 230° | **24** | 106° | **44** | 262° | **64** | 236° | **84** | 136° |
| **5** | 229° | **25** | 84° | **45** | 310° | **65** | 230° | **85** | 338° |
| **6** | 213° | **26** | 78° | **46** | 306° | **66** | 190° | **86** | 240° |
| **7** | 224° | **27** | 98° | **47** | 338° | **67** | 106° | **87** | 141° |
| **8** | 240° | **28** | 118° | **48** | 314° | **68** | 118° | **88** | 118° |
| **9** | 262° | **29** | 102° | **49** | 302° | **69** | 262° | **89** | 262° |
| **10** | 260° | **30** | 82° | **50** | 180° | **70** | 229° | **90** | 314° |
| **11** | 270° | **31** | 128° | **51** | 270° | **71** | 168° | **91** | 262° |
| **12** | 200° | **32** | 172° | **52** | 138° | **72** | 84° | **92** | 152° |
| **13** | 169° | **33** | 112° | **53** | 128° | **73** | 142° | **93** | 102° |
| **14** | 190° | **34** | 118° | **54** | 280° | **74** | 310° | **94** | 292° |
| **15** | 168° | **35** | 142° | **55** | 179° | **75** | 213° | **95** | 302° |
| **16** | 149° | **36** | 148° | **56** | 200° | **76** | 149° | **96** | 260° |
| **17** | 136° | **37** | 136° | **57** | 119° | **77** | 78° | **97** | 144° |
| **18** | 141° | **38** | 262° | **58** | 72° | **78** | 148° | **98** | 82° |
| **19** | 152° | **39** | 292° | **59** | 264° | **79** | 306° | **99** | 294° |
| **20** | 138° | **40** | 294° | **60** | 220° | **80** | 224° | **100** | 332° |

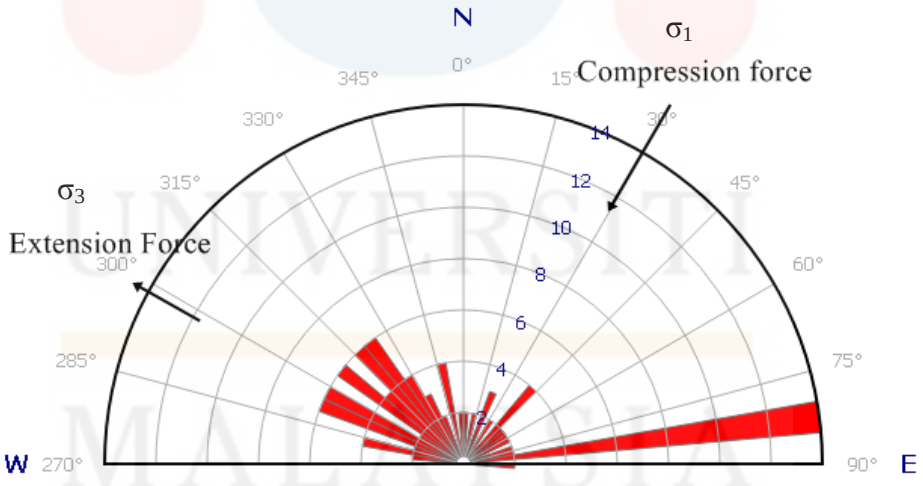


**Figure 4.32** : Rose diagram of location 2

Figure 4.32 shows that there two forces act on the joint. From NE is the compression force, based on the average of two highest reading at 30° and to NW is extension force at 298°, based on 90° angle from the compression force.

**Table 4.6 : Joint sampling reading (location 3)**

| | | | | | | | | | |
|---|---|---|---|---|---|---|---|---|---|
| **1** | 84° | **21** | 82° | **41** | 270° | **61** | 56° | **81** | 62° |
| **2** | 76° | **22** | 130° | **42** | 110° | **62** | 116° | **82** | 76° |
| **3** | 56° | **23** | 156° | **43** | 312° | **63** | 156° | **83** | 82° |
| **4** | 44° | **24** | 258° | **44** | 320° | **64** | 170° | **84** | 104° |
| **5** | 40° | **25** | 50° | **45** | 356° | **65** | 312° | **85** | 280° |
| **6** | 38° | **26** | 92° | **46** | 266° | **66** | 44° | **86** | 38° |
| **7** | 62° | **27** | 82° | **47** | 280° | **67** | 108° | **87** | 100° |
| **8** | 38° | **28** | 56° | **48** | 262° | **68** | 258° | **88** | 156° |
| **9** | 70° | **29** | 276° | **49** | 270° | **69** | 160° | **89** | 112° |
| **10** | 108° | **30** | 288° | **50** | 144° | **70** | 320° | **90** | 262° |
| **11** | 40° | **31** | 280° | **51** | 84° | **71** | 40° | **91** | 70° |
| **12** | 84° | **32** | 264° | **52** | 40° | **72** | 72° | **92** | 122° |
| **13** | 116° | **33** | 160° | **53** | 82° | **73** | 50° | **93** | 276° |
| **14** | 108° | **34** | 160° | **54** | 280° | **74** | 98° | **94** | 132° |
| **15** | 72° | **35** | 98° | **55** | 270° | **75** | 356° | **95** | 108° |
| **16** | 84° | **36** | 140° | **56** | 76° | **76** | 38° | **96** | 92° |
| **17** | 76° | **37** | 104° | **57** | 84° | **77** | 84° | **97** | 288° |
| **18** | 100° | **38** | 112° | **58** | 130° | **78** | 92° | **98** | 224° |
| **19** | 122° | **39** | 132° | **59** | 264° | **79** | 140° | **99** | 144° |
| **20** | 92° | **40** | 224° | **60** | 110° | **80** | 266° | **100** | 140° |

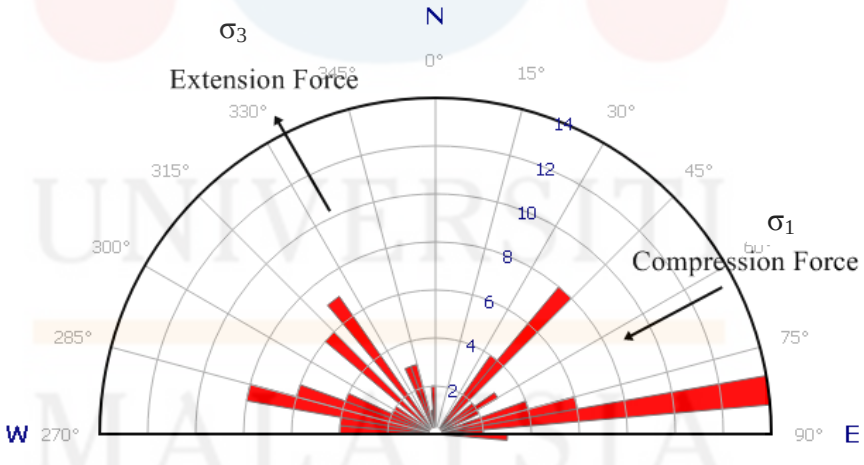


**Figure 4.33** : Rose diagram of location 3

Figure 4.33 shows that there two forces act on the joint. From NE is the compression force, based on the average of two highest reading at 62° and to NW is extension force at 332°, based on 90° angle from the compression force.

**Table 4.7 : Joint sampling reading (location 4)**

| | | | | | | | | | |
|---|---|---|---|---|---|---|---|---|---|
| **1** | 49° | **21** | 47° | **41** | 63° | **61** | 29° | **81** | 24° |
| **2** | 80° | **22** | 10° | **42** | 13° | **62** | 21° | **82** | 52° |
| **3** | 41° | **23** | 21° | **43** | 8° | **63** | 70° | **83** | 74° |
| **4** | 67° | **24** | 10° | **44** | 14° | **64** | 81° | **84** | 61° |
| **5** | 16° | **25** | 13° | **45** | 19° | **65** | 21° | **85** | 40° |
| **6** | 61° | **26** | 69° | **46** | 70° | **66** | 67° | **86** | 54° |
| **7** | 13° | **27** | 81° | **47** | 34° | **67** | 16° | **87** | 30° |
| **8** | 7° | **28** | 50° | **48** | 16° | **68** | 16° | **88** | 49° |
| **9** | 61° | **29** | 36° | **49** | 19° | **69** | 88° | **89** | 47° |
| **10** | 70° | **30** | 28° | **50** | 68° | **70** | 7° | **90** | 63° |
| **11** | 50° | **31** | 47° | **51** | 54° | **71** | 13° | **91** | 29° |
| **12** | 73° | **32** | 82° | **52** | 71° | **72** | 47° | **92** | 52° |
| **13** | 78° | **33** | 52° | **53** | 65° | **73** | 72° | **93** | 80° |
| **14** | 77° | **34** | 33° | **54** | 37° | **74** | 47° | **94** | 10° |
| **15** | 80° | **35** | 8° | **55** | 3° | **75** | 56° | **95** | 13° |
| **16** | 60° | **36** | 44° | **56** | 11° | **76** | 72° | **96** | 21° |
| **17** | 65° | **37** | 75° | **57** | 28° | **77** | 12° | **97** | 74° |
| **18** | 80° | **38** | 21° | **58** | 76° | **78** | 11° | **98** | 41° |
| **19** | 87° | **39** | 11° | **59** | 60° | **79** | 16° | **99** | 21° |
| **20** | 54° | **40** | 13° | **60** | 44° | **80** | 90° | **100** | 8° |

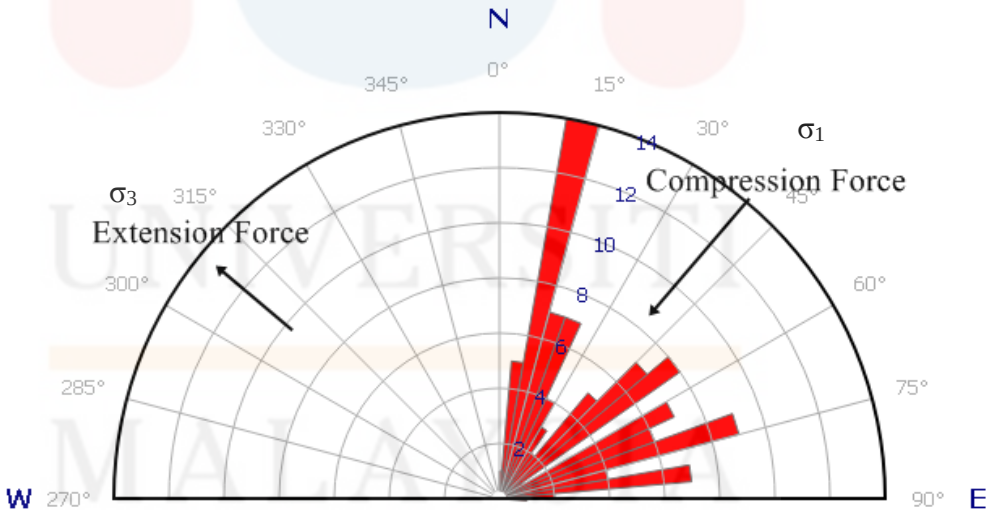


**Figure 4.34** : Rose diagram for location 4

Figure 4.34 shows that there two forces act on the joint. From NE is the compression force, based on the average of two highest reading at 40° and to NW is extension force at 310°, based on 90° angle from the compression force.

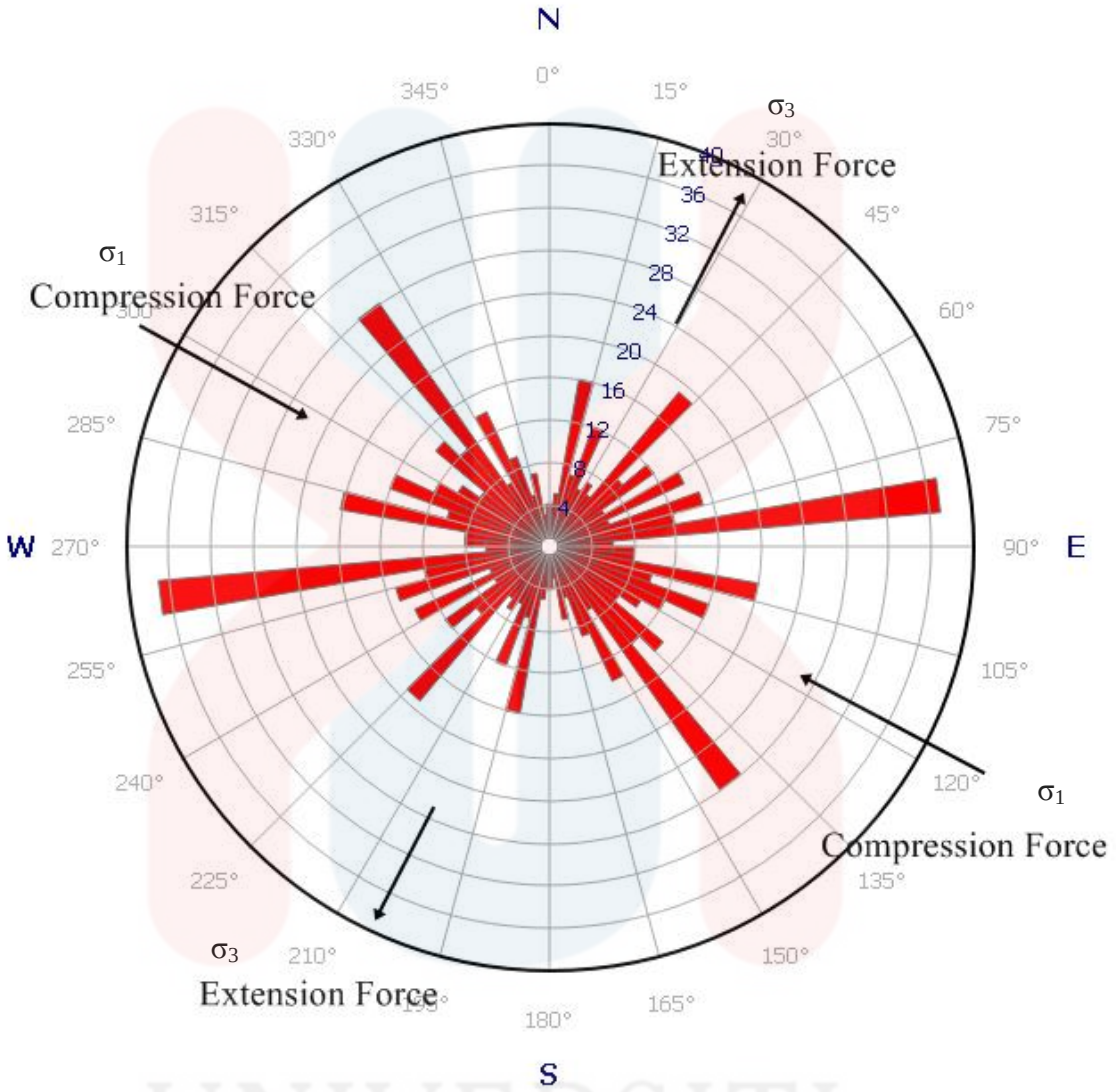


**Figure 4.35** : Rose diagram of all joint sampling data combined

Based on Figure 4.35, these are the results of combination of all joint sampling data. There are two main forces acting in and out of the rose diagram. From NW and ES, the compression force act on the two of the highest reading at 298° and 118° respectively. The extension force from NE at 30° and WS at 205° is results from the 90 ° angle from both of the compression force. The orientation of the highest reading can be said similar the orientation of the lineament, albeit with little deviation.

## 4.5 Historical Geology

The formation at the study area is Gua Musang Formation. The formation age ranges from the Middle Permian to Upper Triassic, covering parts of Palaeozoic era and Mesozoic era (Mohd Shafeea Leman, 2007). The limestone occurs as lenses and forms isolated towers of limestone, and 650 meters thick.

The Paleozoic stratigraphy of the Gua Musang Formation comprises of crystalline limestone interbedded with thin shale, tuff, chert nodules, and sandstone. The limestones at the formation have black and grey variety. This comes from the impurities of carbonaceous, argillaceous and pyroclastic origin.

The historical geology of the study area can be correlated to the type of limestone that can be found on the study area. Examination of hand sample and thin section can give insight of the rock depositional environment, and their past geological conditional ( Ford 1962, etc. )

FYP FSB
UNIVERSITI
MALAYSIA
KELANTAN

# CHAPTER 5

## ELECTRICAL RESISITIVITY IMAGING (ERI) ANALYSIS

### 5.1 Introduction

The survey lines has been done to three different location as shown in Figure 5.2 The location is choosing based on the karst environment of the area. ABEM Terrameter S4000 software is used to measure the resistivity data.

Visual model are made by process called inversion by converting the data obtain from the electrical resistivity profiling. Model from the inversion process is interpreted and the interpretation of the model is guided by using value from Palacky.

Each of materials has its own resistivity value. Figure 5.1 shows that igneous and metamorphic rocks typically have high resistivity values. The resistivity values of these rocks are mainly dependent on the degree of fracturing. Limestone normally has resistivity value of 1 x $10^3$ to 1 x $10^5$ Ωm, whereas water has resistivity value of 10 – 100 Ωm.

The relationship between resistivity and porosity is given by Archie's Law**.** Archie's Law is only applicable if the solid material is non-conducting, such as sand.

$$\rho r = a\ \rho w\ \phi\ -m$$

Where $\rho r$ = rock resistivity, $\rho w$ = fluid resistivity, $a \approx 1$, $m \approx 2$ $\phi$ = fraction of the rock or soil filled with fluid.

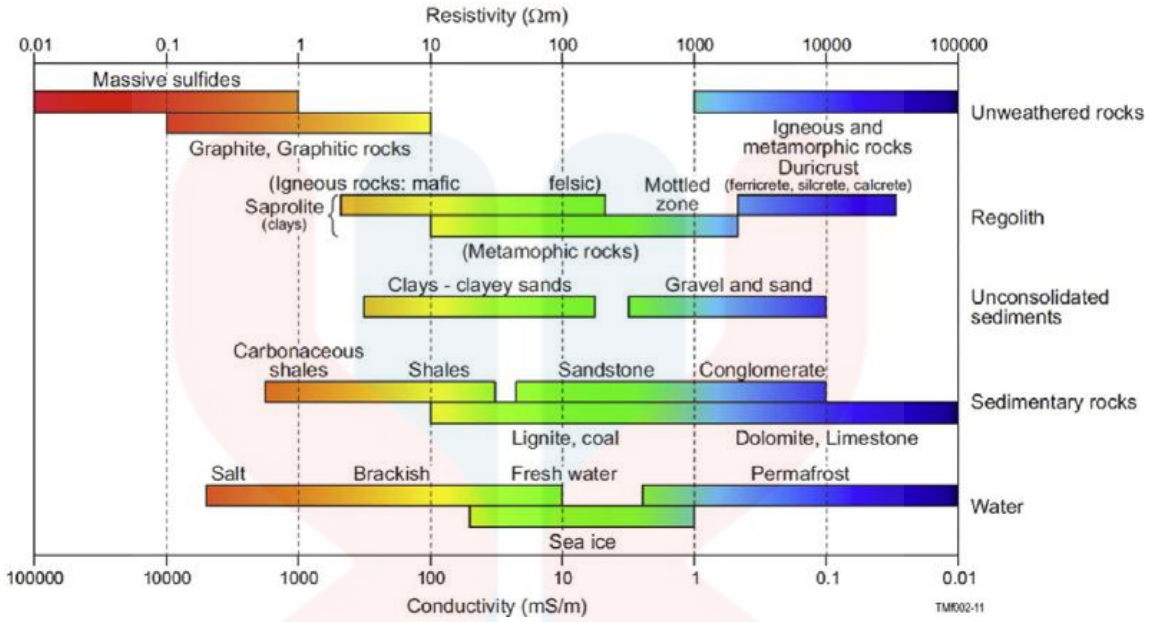


Figure 5.1: The resistivity of rocks, soils and minerals ( from Palacky 1987 )

## 5.2 Electrical Resistivity Profile

There are three electrical resistivity profiles. Each of the profile length is 200 metres. Based on Figure 5.3, the location of each profile are located around Gua Madu. Each profile is labelled as P1, P2, P3 and P4.

There are few parameters when choosing the location for ERI analysis, such as length, within the limestone area, avoiding lamp or phone post and accessibility. The location chosen must be able to accommodate the length of profile in a straight line. Iron metal such as lamp or phone post must be avoided because it can influence the reading of resistivity underground. Accessibility of the preferred location has to be considered in order to run the ERI analysis efficiently in the area.

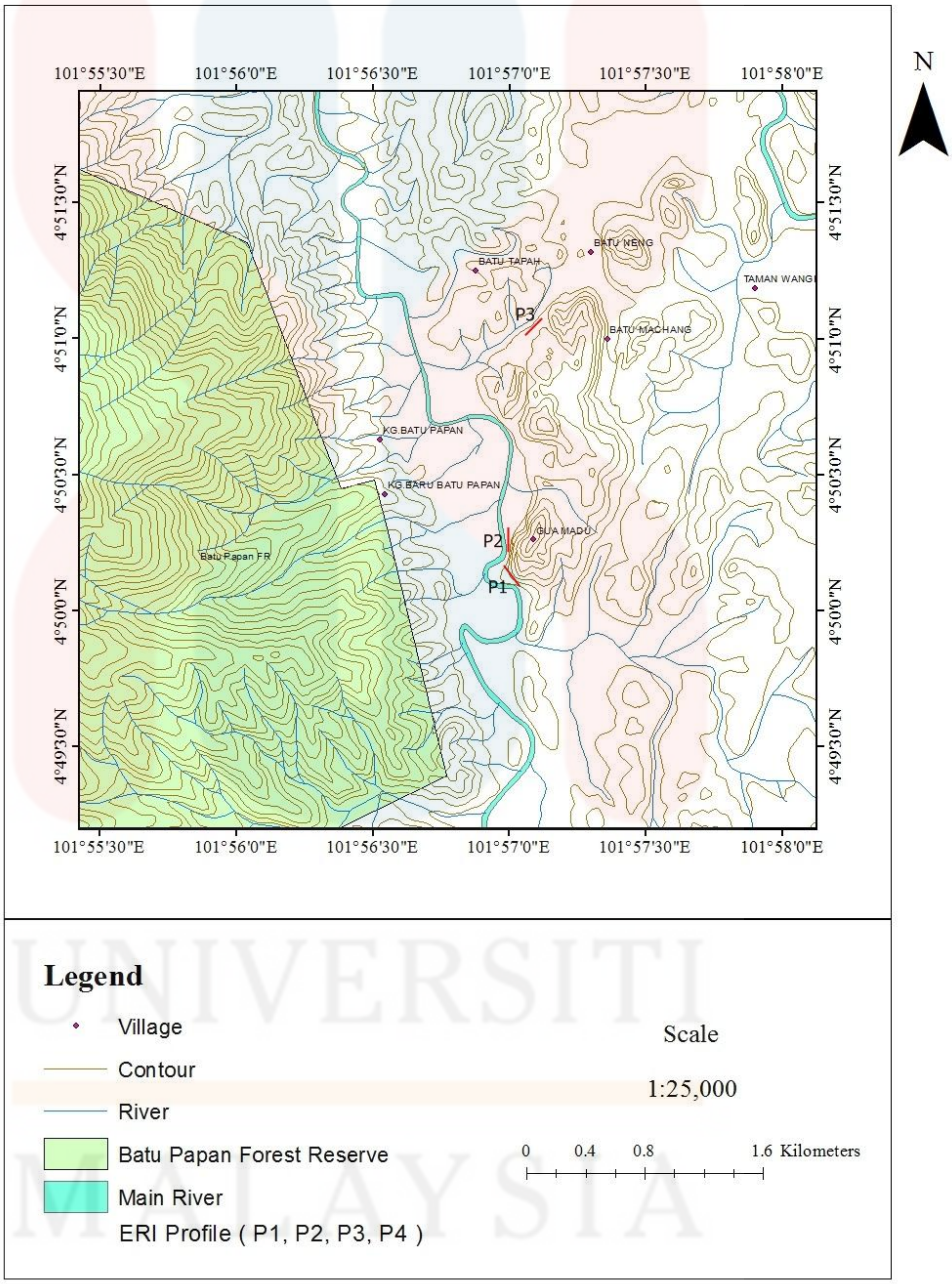


**Figure 5.2** : ERI Profile location of study area

## 5.3 Analysis

The data obtained from the profiling need to process by using computer before it can be analysed. The raw data from the instrument (ABEM Terrameter LS) comes in format of *.s4k and converted by using ABEM Terrameter LS Toolbox software into *.dat format. Process of transferring each data to computer is 30 minutes. Then, the *.dat format file is used in the inversion process by using the software RES2DINV.

First, bad data point is exterminated. In this step, the apparent resistivity data values are displayed in the form of profiles for each data level. This can only be used for data collected using conventional arrays. Data point is considered bad if the point overlap or crosses another line above or below it.

The main purpose of this option is to remove data points that have resistivity values that are clearly wrong. Such bad data points could be due to the failure of the relays at one of the electrodes, poor electrode ground contact due to dry soil, or shorting across the cables due to very wet ground conditions. These bad data points usually have apparent resistivity values that are obviously too large or too small compared to the neighbouring data points (Figure 5.3). The best way to handle such bad points is to drop them so that they do not influence the model obtained.

FYP FSB
UNIVERSITI
MALAYSIA
KELANTAN

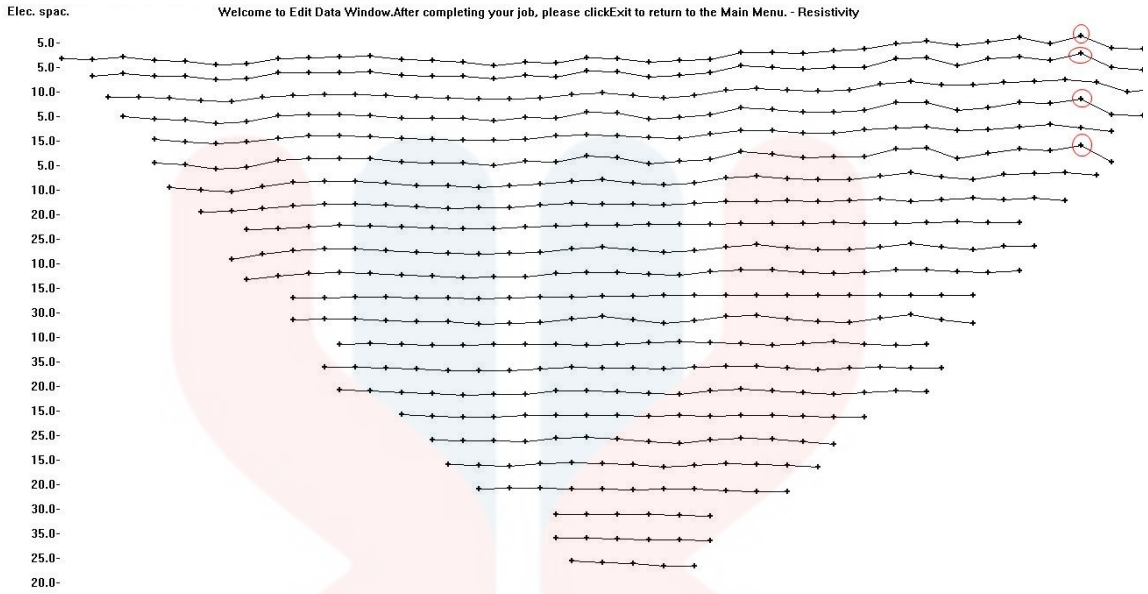


**Figure 5.3** : Example of a data set with a few bad data points.

Next step is the inversion process. Inversion process is done by using least square inversion method in the RES2DINV software. The conventional least-squares method, the standard data constraint will attempt to minimize the square of difference between the measured and calculated apparent resistivity values.

This method gives reasonable results if the data contains random or "Gaussian" noise. However if the data set contains "outlier" data points (where the noise comes from non-random sources such mistakes or equipment problems), this criteria is less satisfactory. The product of inversion is shown in Figure 5.4

FYP FSB
UNIVERSITI
MALAYSIA
KELANTAN

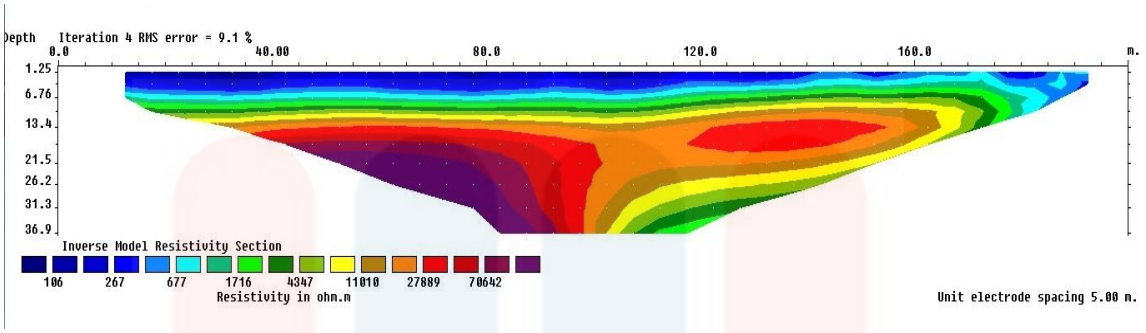


**Figure 5.4** : Product of inversion using least square inversion method

The product had to undergo another process processed if the iteration RMS error is high. The lower the RMS error value, the better the product of inversion. However, too low RMS error number can be produce unrealistic model ( Loke 2014). Based on Figure 5.4, RMS error is 9.1 %. The process that reduces RMS error is called trimming.

By selecting the cut-off error, the data is trimmed. Figure 5.5 shows the trimming window in the RES2DINV software. In the figure, the cut – off error is selected at 60%. Trimming must be done little by little in order to avoid removing too much of the datum point and avoid realistic model.

FYP FSB
UNIVERSITI
MALAYSIA
KELANTAN

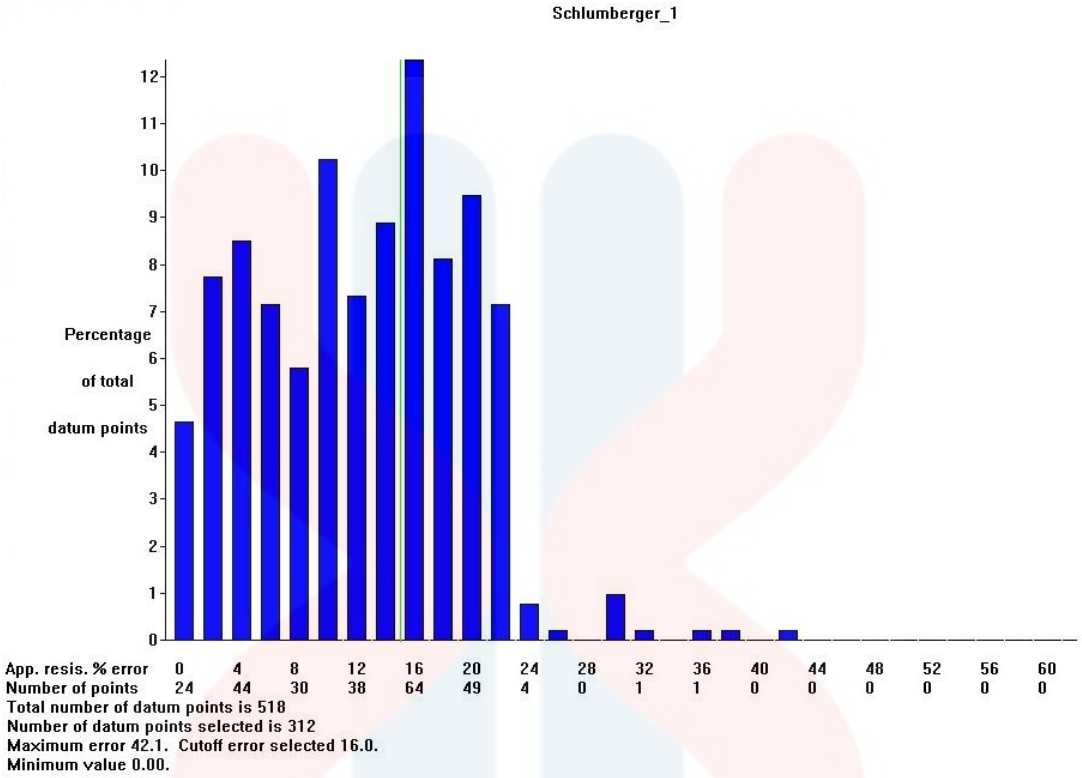


**Figure 5.5** : Trimming with cut-off error selected at 15%

## 5.4 Result

The product of inversion is now complete. Then, the completed inversion is analysed and interpreted to predict the potential limestone geohazard on the subsurface. The analysis is done by referring the value in the inversion model stated by Pallacky (1987). Geological condition of the location can also be related to the inversion model that might cause and produce anomaly.

FYP FSB
UNIVERSITI MALAYSIA KELANTAN

### 5.4.1 P1

The profile line P1 is shown in Figure 5.6. The figure is already marked with dotted lines and corresponding resistivity values. The figure is divided into 3 zones with different resistivity range, zone 1, zone 2 and zone 3. The 3 zones different resistivity range can be attributed to the rock type and water content. P1 on the Figure 5.7 represents the 1st electrode, while P1' represents 20th electrode and P1" represents 41st electrode.

In Figure 5.8, the zone 1 marks area with resistivity value ranging from 79.6 to 800 Ωm. The depth of the zone is surface from 1.25m to 6.76m. This zone is said as unconsolidated sediment saturated with water, hence the resistivity value that corresponds with resistivity range of water. The filed surface condition during the profiling is quite wet and it also raining at that time, which is corresponds with the resistivity value.

Zone 2 marks area with resistivity value ranging from 2589 to 8054 Ωm. The depth of the zone is from 6.76 to 13.4m. This zone can be said as slightly weathered limestone is present, and that corresponds with the range of resistivity value.

Zone 3 marks area with resistivity value ranging from 25541 to 256966 Ωm.. The depth of the zone is from 7m to 36.9m. This zone can be said as massive, unweathered limestone. This massive limestone is also very dry, with zero water content corresponds to high resistivity value.

FYP FSB
UNIVERSITI MALAYSIA KELANTAN

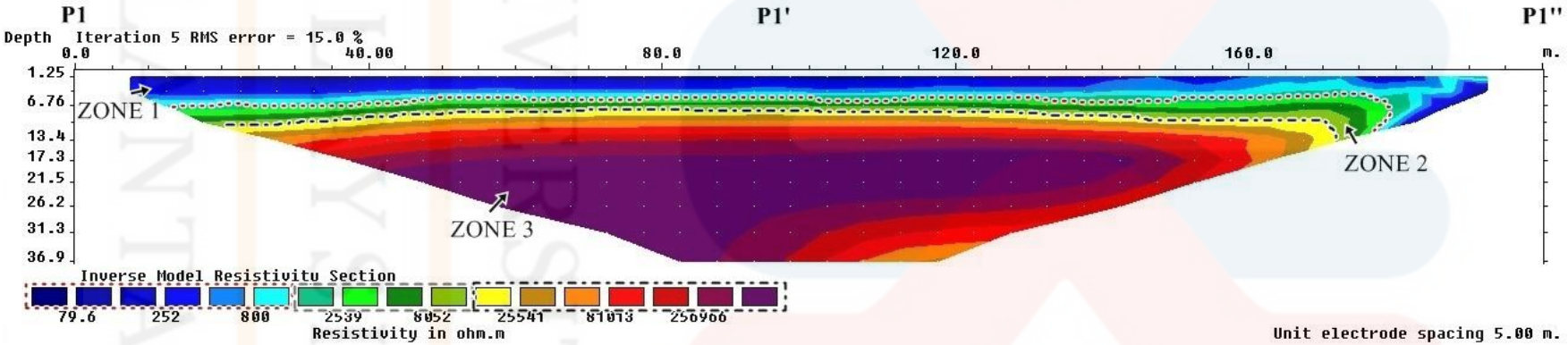


**Figure 5.6** : Resistivity profile P1. P1 indicates the starting point. P1' is the middle point and P1'' indicates end point.



UNIVERSITI MALAYSIA KELANTAN
FYP FSB

### 5.4.2 P2

The profile line P2 is shown in Figure 5.7. The figure is already marked with dotted lines and corresponding resistivity values. The figure is divided into 3 zones with different resistivity range, zone 1, zone 2 and zone 3. The 3 zones different resistivity range can be attributed to the rock type and water content. In Figure 5.8 , P2 represents the 1$^{st}$ electrode, P2' represents 20$^{th}$ electrode and P2" represents the 41$^{st}$ electrode.

In Figure 5.10, zone 1 marks the area with resistivity value from 27.6 to 282 Ωm. The depth of the zone is from 6.76m to 13.4m. This zone can be said as sediment saturated with water, correspond to the resistivity value of water. The zone is very dominant near the surface. The reading corresponds to the surface of profiling, where there are one small river and wetlands in the area.

Zone 2 marks the area with resistivity value from 903 to 2889 Ωm. The zone depth is from 7m to 17.3m. This zone indicates that conglomerate, sandstone and weathered limestone are present.

Zone 3 marks the area with resistivity value from 9244 to 94657 Ωm. The depth of the zone is from 7m to 36.9m. This zone indicates that the fresh, unweathered limestone is present on the area. The limestone is massive and dry, with zero water content based on its high resistivity value.

FYP FSB
UNIVERSITI MALAYSIA KELANTAN

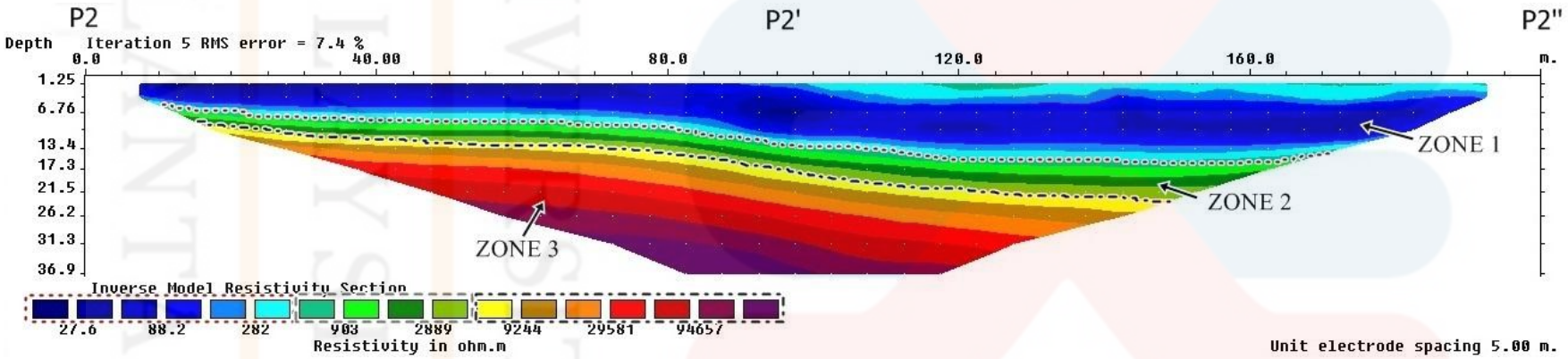


**Figure 5.7**: Resistivity profile P2. P2 indicates the starting point. P2' is the middle point and P2'' indicates end point.



FYP FSB

### 5.4.3 P3

The profile line P3 is shown in Figure 5.8. The figure is already marked with dotted lines and corresponding resistivity values. The figure is divided into 3 zones with different resistivity range, zone 1, zone 2 and zone 3. The 3 zones different resistivity range can be attributed to the rock type and water content. In Figure 5.9, P3 represents the 1st electrode, P3' represents the 20th electrode and P3" indicates the 41st electrode.

In Figure 5.19, zone 1 marks the area of resistivity value from 23.9 to 59.1 Ωm. The depth of the zone is from 1.25m to 21.5m. This zone contain unconsolidated sediment with high content of water, gives it low resistivity value. The zone is appear on the left side and center, which indicates the river and cavities or groundwater is present. The reading corresponds to the surface of profiling, which there are one small river flow underground.

Zone 2 marks area of resistivity value from 92.9 to 146 Ωm. The zone depth is 7m to 17.3m. This zone also contained unconsolidated sediment with high water content, based on the reading of resistivity value.

Zone 3 represents the highest resistivity value, ranging from 290 to 568 Ωm. The zone depth is from 6.76m to 36.9m. This indicates porous limestone with various water content. This zone has highly weathered limestone based on Figure 5.9, that some part of the limestone is separated from the main parent rock due to water seep.

FYP FSB
UNIVERSITI
MALAYSIA
KELANTAN

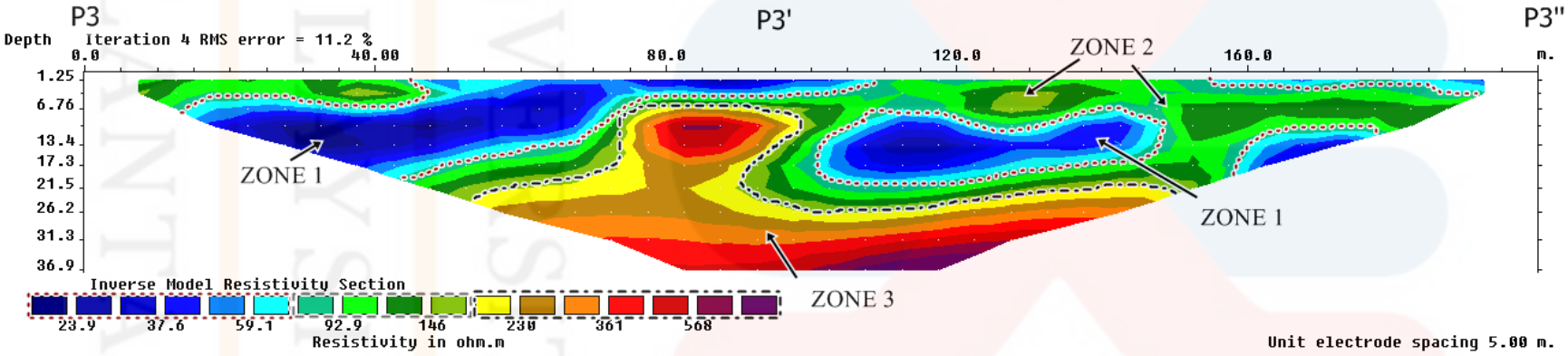


**Figure 5.8** : Resistivity profile P3. P3 indicates the starting point. P3' is the middle point and P3'' indicates end point.

FYP FSB

# CHAPTER 6

## 6.1 Conclusion

The objective of this research is achieved by means of field mapping and electrical resistivity survey, and the result is reported in chapter 4 and 5. The objective of this research is to produce a geologic map of the study area and to predict the limestone geohazard of the area.

The geological map is partially produced with existing data acquired from JUPEM. The map produced is checked and updated by geological mapping. The result of the mapping is reported in chapter 4 and its subchapter.

Subsurface condition of the study area is identifying by using electrical resistivity imaging (ERI) method. ABEM Terrameter SAS 4000 has been use to measure the resistivity. Three resistivity profiles, P1, P2 and P3 have been made and interpret in chapter 5 along with the figure of the resistivity value.

The prediction of limestone geohazard cam be made after the data has been collected by using ERI method. The data is then analyse in chapter 5. Based on the results, P1 and P2 does not have any potential limestone geohazard because of the massive limestone are present with high resistivity value. P3 indicates that potential limestone geohazard is highly present. This is because underground river and groundwater are present, corresponds to the low resistivity value indicates high water content in the area, and may lead to sinkhole.



FYP FSB
UNIVERSITI MALAYSIA KELANTAN

## 6.2 Recommendation

There are few recommendation that can be done to improve the results from electrical imaging resistivity (ERI) method. Seismic methods can be done simultaneously with ERI method to improve the accuracy of results of resistivity on subsurface condition. The length of electrode can be increased from 200 metres to 800 metres to gain more penetration and data in the subsurface. The development of resistivity imaging techniques has been rapid in the last years, so 3D and 4D resistivity method can be used as both are advanced method and can provide more real and accurate data.

FYP FSB
UNIVERSITI
MALAYSIA
KELANTAN

**References**


Avants B., Soodak D., and Ruppeiner G., (1999 ) Measuring the electrical conductivity of the earth, Am. J. Phys. 67 7 87 9 , 593–598

Baweic, W. J. in press. Geologic terranes of Puerto Rico. Geology of Puerto Rico in Geology, Geochemistry, Geophysics, Mineral Occurrences and Mineral Resource Assessment for the Commonwealth of Puerto Rico. USGS Open File Report 98-38.

Bonacci, O.; Ljubenkov, I.; and Roje- Bonacci, T. (2006) Karst flash floods: an example from the Dinaric karst (Croatia), Natural Hazards and Earth System Sciences, vol. 6: 195-203

Boyer, R., and McQueen, J. (1964) Comparison of mapped rock fractures and air photo linear features. Photogrammetric Engineering and Remote Sensing, 30 (4): 630-635.

Braun, O.P.G. (1982) A structural synthesis of Brazil, based on the study of major lineaments derived from remote sensing imagery interpretation. Photogrammetria. 37: 77-108.

Briggs, R P. and Akers, J.P. (1965) Hydrogeologic map of Puerto Rico and adjacent islands. USGS Hydrologic Investigation Atlas HA-197. Washington.

Briggs, R.P. (1964) Provisional geologic map of Puerto Rico and adjacent islands. USGS Misc. Geologic Investigations Map I-392. Scale 1:240,000

Brown, N. (1994) Integrating structural geology with remote sensing in hydrogeological resource evaluation and exploration. I 144-154. Tenth Thematic Conference in Geologic Remote Sensing, San Antonio, TX.

Cardarelli E., Di Filippo G., Tuccinardi E., (2006a) Electrical resistivity tomography to detect buried cavities in Rome: a case study. Near Surface Geophysics, 4, 387–392.

Cardarelli E., Fischanger F., (2006b) 2D data modelling by electrical resistivity tomography for complex subsurface geology. Geophysical Prospecting, 54, 121–134.

Chalikakis K., Plagnes V., Guerin R., Valois R., Bosch F. P., (2011) Contribution of geophysical methods to karst-system exploration: an overview. Hydrogeology Journal, 19, 1169–1180.

Charlton, R. (2008) Fundamentals of Fluvial Geomorphology, Routledge, N.Y., pp. 1-20.

Cook K. L., Van Nostrand R. G., (1954) Interpretation of resistivity data over filled sinks. Geophysical Prospecting, 21, 716–723.




FYP FSB
UNIVERSITI MALAYSIA KELANTAN

Dutta N., Bose R., Saikia B., (1970) Detection of solution channels in limestone by electrical resistivity method. Geophysical Prospecting, 18, 405–414.

E. S. Robinson and C. Coruh, (1988) Basic Exploration Geophysics , Wiley, New York,.

Fatihah, R. M, (2002) The Characteristic and Origin of the Tropical Limestone Karst of the Sungai Perak Basin, Malaysia. University of Malaya: 22-23.

Greenfield R. J., (1979) Review of geophysical approaches to the detection of karst. Bull. Assoc. Eng. Geol., 16, 393–408

Griffiths, D. H. and Barker, R. D. (1993) Two-dimensional resistivity imaging and modeling in areas of complex geology. 211–226.

Griffiths, D.H. and Turnbull, J. (1985) A multi-electrode array for resistivity surveying. First Break 3 (No. 7), 16-20

Howard, A.D. (1967) Drainage analysis in geologic interpretation: a summation. American Association of Petroleum Geologists Bulletin, 51, pp. 2246-2259.

Hutchison C.S., (1973). Metamorphism. In D.J. Gobbett and C.S. Hutchison, (Eds.) Geology of the Malay Peninsula. Wiley-Intersc., N.Y., 253-303

Jennings, J. N., (1982). Principle and Problems in Karst History, Helicite, vol. 20, no.2: 37-51.

Kannan, R.C. (1999). Designing foundations around sinkholes", Engineering Geology 52, 75-82.

Kaufmann, O. and Quinif, Y. (2002) Geohazard map of cover-collapse sinkholes in the 'Tournaisis' area, southern Belgium, Engineering Geology, vol. 65, Issues 2-3: 117-124

Keller G.V. and Frischknecht F.C. (1966) Electrical methods in geophysical prospecting.

Keqiang, H.; Dong, G.; Wen, D.; and Ronglu, W. (2007) The effects of karst collapse on the environments in north China, Environmental Geology, Springer Berlin/ Heidelberg, vol.52, no.3: 449-445.

Lambert, D. (1998) The Field Guide to Geology. Checkmark Books. pp. 130-131.

Lattman, H. and Parizek, R. (1964) Relationship between Fracture Traces and the Occurrence of Ground Water in Carbonate Rocks. Journal of Hydrology, 2, 73-91.

FYP FSB
UNIVERSITI MALAYSIA KELANTAN

Loke, M.H., Barker, R.D. (1996a) Rapid least-squares inversion of apparent resistivity pseudosections by a quasiNewton method. Geophysical Prospecting44 (1), 131–152.

Militzer H., Rosler R., Losch W. (1979) Theoretical and experimental investigations for cavity research with geoelectrical resistivity methods. Geophysical Prospecting, 27, 640–652.

Mohd Shafeea Leman, Kamarulzaman Abdul Ghani, Ibrahim Komoo & Norhayati Ahmad (eds.), (2007). Langkawi Geopark. Lestari UKM Publication, Bangi, 114 pp.

O'Leary, D.W. Freidman, J.D., and Pohn, H.A. (1976). Lineament, linear, lineation: Some proposed new definitions for old terms. Geological Society of America Bulletin. 87:1463-1469.

Oldenburg, D.W. and Li., Y. (1999) Estimating depth of investigation in dc resistivity and IP surveys. Geophysics, 64, 403-416

Oldenburg, D.W., Li, Y. (1994) Inversion of induced polarization data. Geophysics 59, 1327–1341.

Palacky, G.V. (1987), Resistivity characteristics of geologic targets, in Electromagnetic Methods in Applied Geophysics, Vol 1, Theory, 1351

Pergamon Press Inc., Oxford.

Pidwirny, M. (2006) The Drainage Basin Concept. Fundamentals of Physical Geography, 2nd Edition http://www.physicalgeography.net/fundamentals/10aa.html

R. H. Parker and A. B. L. Whittles (1970) Introduction of special topics (geo-Physics) through the use of physics laboratory projects, Am. J. Phys. 38, 65–67.

Reynolds J. M. (1997) An Introduction to Applied and Environmental Geophysics, Wiley, New York

Ritter, M.E. (2003) The Physical Environment: an Introduction to Physical Geography. http://www.uwsp.edu/geo/faculty/ritter/geog101/textbook/title_page.html

Shu, Y.K. (1986). Investigations on land subsidence and sinkhole occurrence in the Klang Valley and Kinta Valley in Peninsular Malaysia. In: Proc. LANDPLAN H Conf., K.L., 15-28.

Shu, Y.K., and Lai, K.H. (1980) Rockfall at Gunung Cheroh, Ipoh. Geological Survey Malaysia, Geological Papers, 3: 1-9.

Simon, D.F. and Gerald, C.N. (2004) The morphology and formation of floodplain-surface channels, Cooper Creek, Australia. Geomorphology, 60, pp. 107-126.



FYP FSB
UNIVERSITI MALAYSIA KELANTAN

Tan, B.K.(1988) Geologi kejuruteraan kawasan sekitaran Ipoh, Perak. (Engineering geology of the Ipoh area, Perak). Laporan Akhir Projek Penyelidikan No.7/86, Sept. 1988, UKM, 74 pp.

Telford, W.M., Geldart, L.P., and Sheriff, R.E. (1990) Applied Geophysics, 2nd Edition, Cambridge University Press, Cambridge.

Thomas B., Roth M. J. S. (1999) Evaluation of site characterization methods for inkholes in Pennsylvania and New Jersey. Eng. Geol., 52, 147–152.

Tjia, H.D., Harun, Z. (1985). Regional structures of Peninsular Malaysia. Sains Malaysian 14, 95-107.

Tsourlos, P. (1995) Modelling, interpretation and inversion of multielectrode resistivity survey data. Ph.D. dissertation, Dept. of Electronics, University of York, York, U.K. 315pp.

Twidale, C.R. (2004) River patterns and their meaning. EarthScience Reviews, 67 (3-4), pp. 159-218.

Vincenz A. (1968) Resistivity investigations of limestone aquifers in Jamaica. Geophysics, 33, 980–994.

FYP FSB

UNIVERSITI
MALAYSIA
KELANTAN